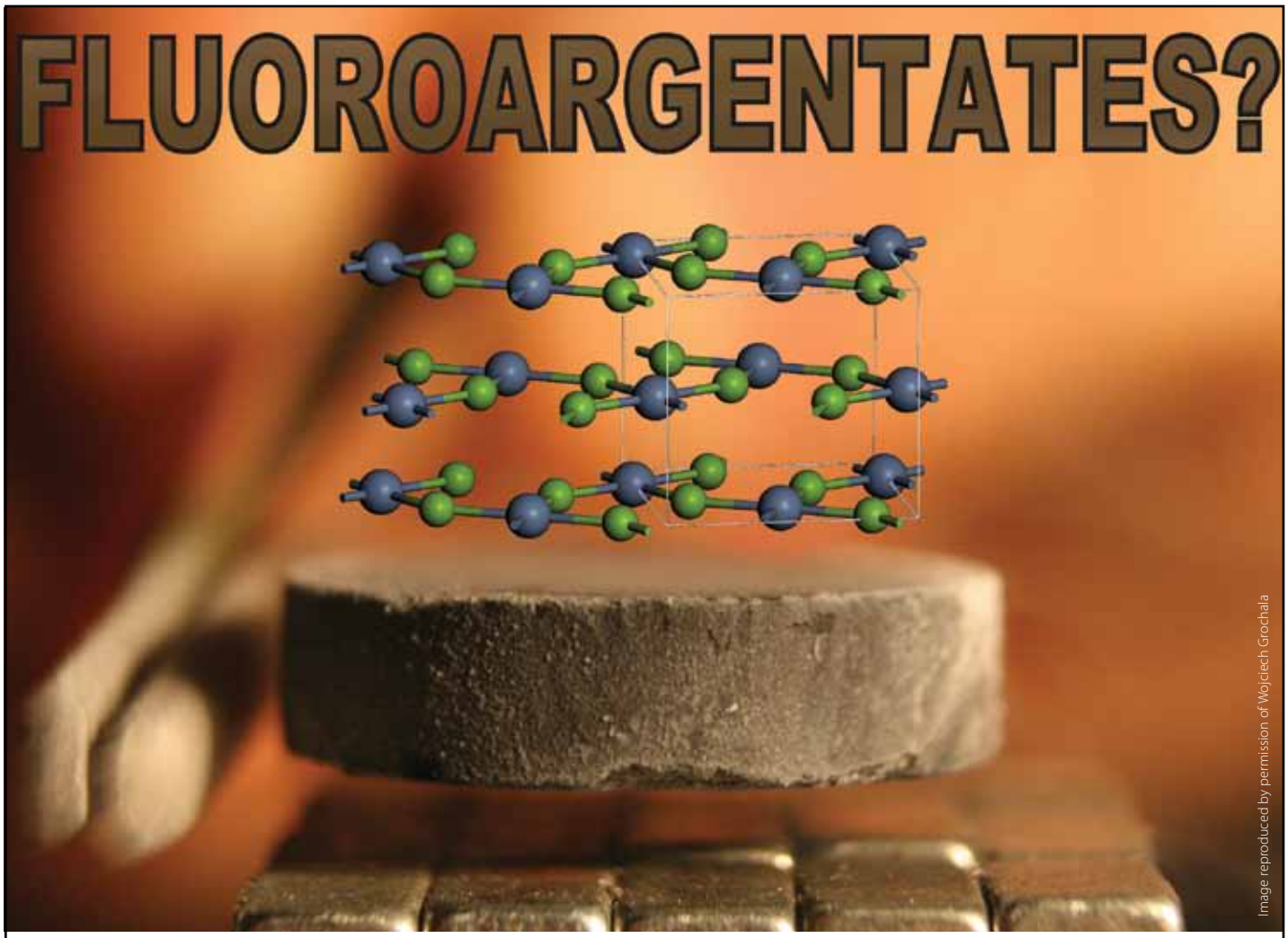

Image reproduced by permission of Wojciech Grochala

Showcasing research from Dr Wojciech Grochala at Laboratory of Technology of Novel Functional Materials, ICM and Faculty of Chemistry, University of Warsaw, Poland, within the TEAM Programme of the Foundation for Polish Science.

Title: The theory–driven quest for a novel family of superconductors: fluorides

Fluorine, the most electronegative among all bond-forming elements, usually forms ionic solids which are electronic insulators. Here, attempts are described to design and synthesize a novel family of superconductors based on extremely reactive derivatives of silver and fluorine: fluoroargentates (II). These fascinating materials share lots of common features with oxocuprates (II).

As featured in:

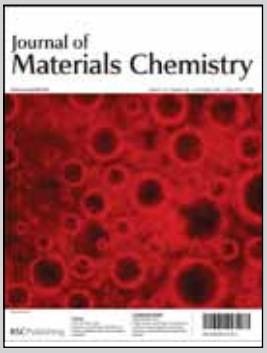

See Wojciech Grochala, *J. Mater. Chem.*, 2009, **19**, 6957

RSC Publishing

www.rsc.org/materials

Registered Charity Number 207890

The theory-driven quest for a novel family of superconductors: fluorides†

Wojciech Grochala*[ab]

Received 2nd March 2009, Accepted 6th May 2009
First published as an Advance Article on the web 29th June 2009
DOI: 10.1039/b904204k

Due to the enormous electronegativity of fluorine, the vast majority of binary and higher inorganic fluorides are high-melting large-band-gap electronic insulators, which are transparent in the visible region of the electromagnetic spectrum. Rare examples of metallic fluorides are known, but valence orbitals of F marginally participate in the electronic transport in these compounds. In this account we describe recent theory-driven attempts to turn unusual fluorides of divalent silver – called fluoroargentates(II) – into a novel class of high-temperature superconductors.

1 Introduction

Fluorine is by all means an unusual chemical element. Sometimes called the '*Tyranosaurus Rex of chemicals*' or the '*Hell-Cat of chemistry*', fluorine reveals its uniqueness by forming connections to virtually all elements capable of chemical bond formation. Bonds between F and metallic elements have substantially ionic character, which is more pronounced than for all other bonds formed by these electropositive elements. In consequence, F stabilizes high oxidation states of metals and nonmetals, a feature which allowed F to play a major role in the Manhattan project (uranium enrichment *via* diffusion of $^{235}UF_6$ and $^{238}UF_6$ in the gas phase). On the other hand, the same feature made possible the preparation of the first 'noble' gas compound, $XePtF_6$, in 1962,[1] and of the first – and so far the only – genuine connection of Ar, HArF, in 2000.[2,3] Such advances further encouraged theoreticians to hypothesize about other unusual connections, such as $Hg(IV)F_4$[4] or $Ir(VII)F_7$.[5] Connections of F to nonmetals are also atypical. For example, the C–F and Si–F bonds are distinctly different from any other bonds formed by carbon and silicon, and extremely difficult to activate under modest conditions. On the other hand, Sb(V) shows such enormous affinity to fluorine that SbF_5 is *the* most potent binary acceptor of a fluoride anion;[6] this in turn makes possible some astonishingly beautiful chemistry to be realized with HF/SbF_5, the most superacidic medium available.[7–9]

The Mulliken electronegativity of F ($\chi_M \approx (I_P + E_A)/2$, where I_P is the first ionization potential of an isolated atom, and E_A its electron affinity) equals 10.42 eV, and is surpassed only by two chemically silent noble gases (Ne 10.79 eV and He 12.30 eV), leaving all other electronegative nonmetallic challengers far behind (Cl 8.30 eV, Ar 7.88, O 7.54 eV, Kr 7.00 eV, see Fig. 1).[10] Most of the physicochemical features of various fluorinated

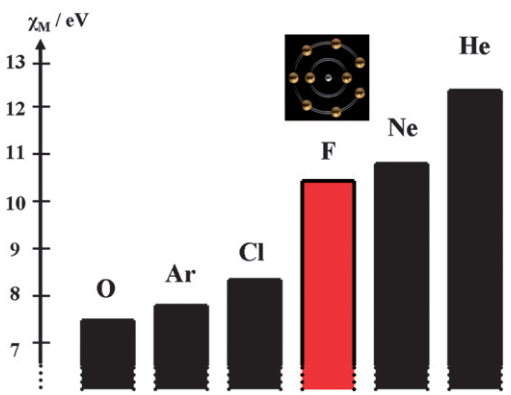

Fig. 1 Illustration of the Mulliken electronegativity, χ_M, of the six most electronegative chemical elements: He, Ne, F, Cl, Ar and O.[10]

[a]*Laboratory of Intermolecular Interactions, The Faculty of Chemistry, The University of Warsaw, Pasteur 1, Warsaw, Poland. E-mail: wg22@cornell.edu; Fax: +48 22 8222309; Tel: +48 22 8220211 x. 276*
[b]*Laboratory of Technology of Novel Functional Materials, Interdisciplinary Centre for Mathematical and Computational Modelling, University of Warsaw, Pawińskiego 5a, 02106 Warsaw, Poland; Fax: +48 22 5540801; Tel: +48 22 5540828*

† This feature paper is dedicated to my dear teacher and trusted friend, Professor Lucjan Piela, on his 65th birthday.

Wojciech Grochala

Wojciech Grochala was born in 1972 in Warsaw, Poland, where he received his MSc, PhD and DSc from the University of Warsaw. Initially a spectroscopist, he felt the magic spell of molecular orbitals during his postdoc with Roald Hoffmann in Ithaca (Cornell, USA) and then fell in love in inorganic and fluorine chemistry while working with Peter P. Edwards (then at Birmingham, UK). Inorganic solid-state chemistry and mountaineering are Wojciech's real passions. His scientific interests encompass noble gas and transition metal chemistry, superconductivity and vibronic coupling, quantum modeling of solids and molecular materials, hydrogen and energy storage, hydrogen transfer catalysis, applications of high pressures in chemistry, molecular devices, unusual oxidation states of the chemical elements, and more. He now heads the Laboratory of Technology of Novel Functional Materials, a joint enterprise of the ICM and of the Faculty of Chemistry at the University of Warsaw.

compounds are thus a straight consequence of the unsurpassed electron-withdrawing properties of F, which probably must be treated as a kind of *force majeure* exerted by F upon all atomic partners in its vicinity. F has a voracious appetite for grabbing electrons from other atoms: first of all the demands of F must be satisfied to the fullest, with the miserable scraps being left for partitioning among the remaining elemental constituents.

The chemical properties of fluorine and its compounds are so different from those of their non-fluorinated analogues that it often excludes the former from many important applications. For example, ammonia and non-fluorinated amines, be they aliphatic or aromatic, are pretty strong Lewis bases, which are ready to form complexes with most metal cations. But surfing through the inorganic structural databases you will not find a single example of a metal cation coordinated by a perfluorinated amine, such as NF_3 or pentafluoropyridine, C_5F_5N. In addition, while NH_3, $N(C_2H_5)_3$ and pyridine are readily soluble in water at all proportions, their perfluorinated analogues do not show the slightest tendency to dissolve, and $N(C_2F_5)_3$ is not miscible with the HSO_3F superacid (!).[11] Fluorine is indeed different from other elements! It is extremely difficult to turn the horrifying Mr. Hyde into a polite Dr. Jekyll but maybe, instead of unsuccessfully trying this, one could rather employ Mr. Hyde for some worthy purpose, not just *despite* F's enormous electron-withdrawing power but precisely *because* of it?

In this feature article we would like to discuss in more detail one such attempt – which has not yet concluded with a 'happy ending' – namely to generate high-temperature (high-T_C) superconductivity in certain inorganic fluoride materials. The theoretical and experimental research described here – recently quite intense – is centered on quite exotic fluoroargentates(II), which are strikingly similar in many aspects to the well known superconducting oxides of copper. But first a brief introduction is needed to the fascinating phenomenon of superconductivity and a short description of the single known family of high-T_C superconductors (SCs) – oxocuprates – and to the role of vibronic effects in these materials.

The plan of the paper is as follows: in section 2 we introduce the reader to the known families of SCs. Section 3 is devoted to the most successful SCs, oxocuprates, and one chemical model of superconductivity (Burdett's model). This model constitutes the basis for our search for novel families of fluoride SCs. In section 4 we describe more general considerations on the strength of vibronic coupling in chemical systems, which allow for identification of fluorine as a key element for high-T_C Bardeen–Cooper–Schrieffer (BCS) mechanism-driven superconductivity. The properties of substantially covalent fluorides are briefly reviewed in section 5. Section 6 is devoted to unusual fluorides of divalent silver.

2 High-, medium- and low-T_C superconductivity

2.1 The discovery of superconductivity in brief

In two years we will celebrate the centenary of the discovery of superconductivity by the Dutch physicist, Heike Kamerlingh Ohnes. On one day in 1911 an excited coworker of Ohnes, Jacob Clay, ran to his tutor's office and announced that 'the resistivity of mercury has disappeared'. Ohnes, suspecting a short circuit or simply a mistake, ordered him to repeat the measurements. The result was confirmed.[12] This story, which began so inconspicuously, has resulted so far in the award of seven Nobel Prizes in physics for the wonderful discoveries made in the field of superconductivity and in the related field of superfluidity.[13]

Another groundbreaking discovery was made in 1933, when Walther Meissner and Robert Ochsenfeld showed that a superconducting material repels a magnetic field due to the induction of supercurrents at the surface of the superconductor.[14] This behaviour, unique to superconductors and known as the Meissner effect, together with an *unmeasurable* DC resistivity, constitutes the most fundamental feature of a superconducting state of matter – and leads to many important applications.

2.2 Families of superconductors

The majority of known superconductors are elemental metals (the previous record T_C value, 9.25 K for Nb, was surpassed in 2001 by 15 K for aligned single-walled carbon nanotubes[15]), and intermetallic alloys (8 K for Ba_8Si_{46},[16] 18 K for the recently discovered LiFeAs,[17] 18.5 K for $PuCoGa_5$,[18] 23 K for YPd_2B_2C[19]). This family also includes elemental (11.2 K for B at 250 GPa,[20] 17.3 K for S at 190 GPa[21]), covalent (17 K for SiH_4 at 96 GPa[22]) and ionic (1.5 K for CsI at 206 GPa[23]) semi-metals and insulators, which have been forced into a superconducting state by use of ultra-high pressures (often surpassing 10^6 atm). The appearance of superconductivity and/or an increase in T_C are also frequently seen for compressed metals (2 K for Fe at 22 GPa,[24] 20 K for Li at 48 GPa,[25] 19.6 K for Sc at 106 GPa,[26] 25 K for Ca at 161 GPa[27]). The record T_C value in the 'elements

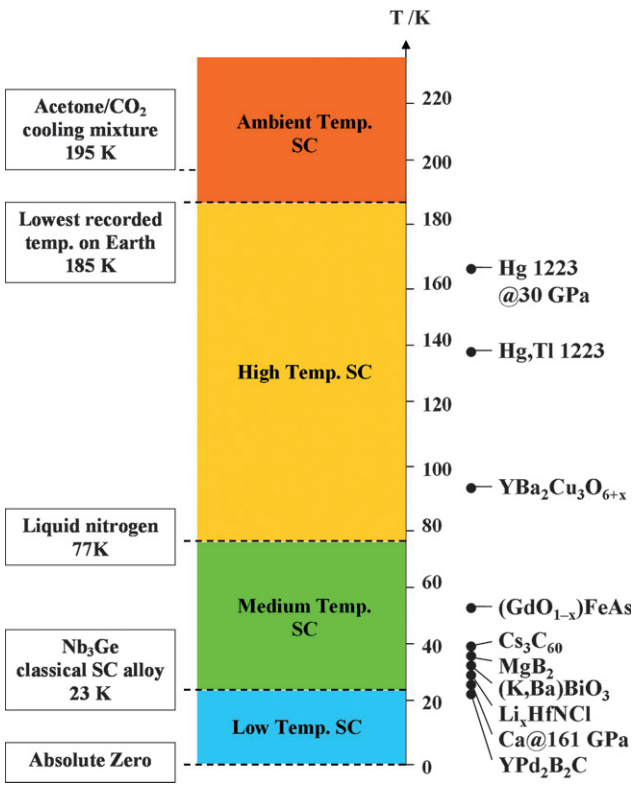

Fig. 2 Position of several important families of superconductors within the low-, medium-, high-, and ambient-T_C categories.

and alloys' family has long been held by Nb_3Ge (23.2 K),[28] and for historic reasons this value marks a borderline between low- and medium-T_C superconductivity (Fig. 2). Very recently, a new record for this family has been set by $(Eu_{0.5}K_{0.5})(FeAs)_2$ (32 K).[29]

The largest T_C values are seen for connections between metals and semi-metals (B) or non-metals (C, N, O, Cl). They are exemplified by 25.5 K for Li_xHfNCl,[30] 30 K for $Ba_{0.6}K_{0.4}BiO_3$, 39 K for MgB_2,[31] 40 K for Cs_3C_{60},[32] and around 52–53.5 K for $(MO_{1-x})FeAs$ and $M(O_{1-x}F_x)FeAs$ (M = Sm, Pr, Gd, *etc.*).[33] The T_C values for all these families fall into what might be called a medium-T_C regime (Fig. 2), extending between 23.2 K and 77.4 K (b.p. of nitrogen).

Finally, only one family of superconductors is found at $T > 77.4$ K, *viz.* the oxocuprates. Its first low-T_C member, $La_{2-x}Ba_xCuO_4$, was discovered in 1986,[34] laying the ground for the enormous experimental and theoretical research which followed. The 'magic barrier' of liquid nitrogen temperature was conquered in 1987 ($YBa_2Cu_3O_{6+x}$, 93 K[35]), and $Hg_{1-x}Tl_xBa_2Ca_2Cu_3O_{8+\delta}$ (138 K) holds the current record value at ambient pressure.[36] An even higher T_C of 164 K has been recorded for the compound known as Hg1223 at high pressure.[37] Unfortunately, the record T_C has not been improved upon for nearly two decades, nor does it approach the lowest recorded temperature on Earth, 185 K – above which extends what we might perhaps call the 'cheap chemical refrigerants' – let alone an 'ambient-T_C' regime (Fig. 2).

It does not take a particularly perceptive analyst to observe that the presence of highly electronegative nonmetals, notably oxygen, seems to be a necessary precondition for achieving high T_C values. This naturally raises a question that could even higher T_C values could be obtained for novel materials based on the even more electronegative elements: chlorine and fluorine? We will return to this important issue in the forthcoming sections.

Summarizing this section, a *multitude* of low-T_C superconductors, *several*, often exotic, families in the medium-T_C regime and just *one* genuinely high-T_C family, oxocuprates, are currently known. Let us thus devote some space to the most successful materials, oxides of copper.

3 High-T_C superconductivity in doped oxocuprates(II)

3.1 Oxocuprate SCs in brief

Oxocuprates(II), *i.e.* ternary and multinary oxides of divalent copper such as La_2CuO_4 or $CaCuO_2$, constitute the parent compounds of all known oxocuprate SCs. The presence of the $[CuO_2]$ layers – usually flat or only slightly puckered – is their most typical structural feature (Fig. 3) and is responsible for the appearance of superconductivity.[38] Generation of superconductivity in these layered compounds requires charge doping; this is realized in most cases by partial chemical substitutions (for example, La(III)→Ba(II) for La_2CuO_4) and/or by introduction of vacancies (as for $(Ca_{1-x}Sr_x)_{1-y}CuO_2$). The vast majority of oxocuprates are hole-doped, thus formally these are intermediate-valence Cu(II)/Cu(III) compounds.

The Cooper pairs responsible for superconductivity bear a positive charge, $2h^+$. Only a few examples are known of electron-doped phases (such as $Nd_{2-x}Ce_xCuO_4$ achieved *via* a Nd(III)→Ce(IV) substitution,[39] $Sr_{1-x}La_xCuO_2$ synthesized at high pressure,[40] or $Li_xSr_2CuO_2Br_2$ accessed *via* electrochemical Li doping[41]) which formally correspond to the Cu(II)/Cu(I) systems; the true nature of charge carriers in these materials ($2e^-$ *vs.* $2h^+$) has been disputed.[42] Regardless of the method of doping, extra carriers do not localize as distinct defects of the crystal lattice (*i.e.* Cu(III) or Cu(I)) but are delocalized over the entire $[CuO_2]$ sheets. The electronic states at the Fermi level are composed mostly of the heavily mixed $3d(x^2-y^2)_{Cu}$ and $2p(x,y)_O$ states.

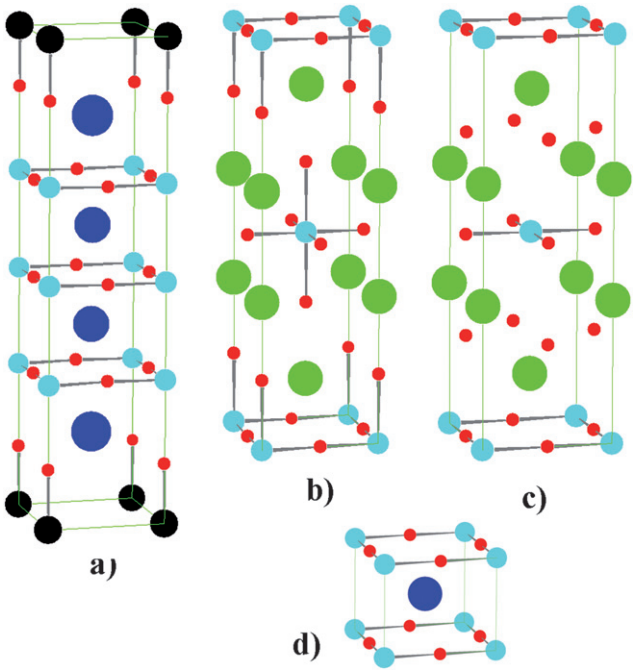

Fig. 3 Comparison of crystal structures of four oxocuprate SCs: (a) the record-holding Hg1223, an intergrowth of $CaCuO_2$ perovskite and $BaHgO_2$, (b) T structure of the first oxocuprate SC, $(La,Ba)_2CuO_4$, (c) T′ structure of the first e^--doped SC, $(Nd,Ce)_2CuO_4$, (d) defect-containing perovskite structure of infinite layer SCs, $(Sr,Ca)_{1-x}CuO_2$ or $(La,Sr)_{1-x}CuO_2$. Cu – light blue, O – red, Hg – black, Ca, Ba – dark blue, La, Nd – green spheres.

The presence of substantial numbers of 'oxygen holes', *i.e.* charge carriers with a predominant $2p_O$ character, has been postulated from near-edge X-ray absorption[43] and high-resolution XPS measurements,[44] and subsequently discussed in numerous papers.[45] Thus, to some approximation, it is fair to discuss a 'metallic oxygen' sublattice in the $[CuO_2]$ sheets. Experimental evidence for the subtle redox equilibrium:

$$Cu^{3+} + O^{2-} \rightleftharpoons Cu^{2+\bullet} + O^{-\bullet} \quad (1)$$

which may be shifted even farther with an increase of temperature:

$$2\,Cu^{3+} + O^{2-} \rightleftharpoons 2\,Cu^{2+\bullet} + \tfrac{1}{2}\,O_2 \quad (2)$$

comes from studies of low-temperature annealing and thermal decomposition of these materials. The majority of oxocuprate SCs spontaneously absorb elemental O_2 when annealed, but they

lose excess dioxygen when heated slightly above 400 K in the stream of an inert gas.[46] An alternative related equilibrium:

$$Cu^{2+\bullet} + O^{2-} \rightleftharpoons Cu^{+} + O^{-\bullet} \quad (3)$$

is more general and representative of all cuprates, since it emphasizes the fact that the Cu^{3+}-free, electron-doped SCs also exhibit substantial covalence of the Cu–O sublattice and that these materials may be prepared by heating of Cu^{2+}-containing precursors *via* oxygen loss:

$$2\,Cu^{2+\bullet} + O^{2-} \rightleftharpoons 2\,Cu^{+} + \tfrac{1}{2}\,O_2 \quad (4)$$

We will return to these important redox reactions in the forthcoming sections.

The presence of heavy elements M from the d- or p-block of the Periodic Table (such as M = Au, Hg, Tl, Pb or Bi) in the crystal structure of oxocuprates usually increases the value of T_C. This effect can be traced back to the substantial relativistic stabilization of the 6s shell, which allows these elements to form strong and fairly covalent bonds with oxide anions (this is also one of the reasons for their toxicity in living organisms – a linear plot of T_C *vs.* the lethal dose of a given SC material has even been derived). Indeed, numerous oxo-salts of the Group 1 and Group 2 cations, such as aurates(I) and (III), mercurates(II), thallates(III), plumbates(II) and (IV) and bismuthates(III) and (V), have been synthesized in the past. Formation of the somewhat covalent M–O bonds in the 'charge reservoir' layers of oxocuprate SCs noticeably increases the density of states at the Fermi level and thus facilitates the transition into the superconducting state.

The presence of heavy elements is not necessary to achieve high-T_C superconductivity, as testified by the defected perovskite $(Ca_{1-x}Sr_x)_{1-y}CuO_2$ with its spectacular T_C of 110 K. The hole-doped slightly nonstoichiometric $CaCuO_2$ (Fig. 3) must thus possess all the essential features which lead to superconductivity *via* intraplane and interplane coupling. The former engages the in-plane Cu–O stretching and deformation modes and is crucial for superconductivity, while the latter further enhances the value of T_C *via* impact of the bond-buckling (planar symmetry-breaking) phonons.

3.2 The 'magic Cu–O bond length'

Since the early days of high-T_C superconductivity, various attempts have been made to correlate the T_C value with other physicochemical parameters. These efforts aimed at a better understanding of the most important factors influencing the spectacular performance of the cuprates, and at further increasing the T_C values.

One particularly intriguing structure–property relationship, linking the T_C value with the in-plane Cu–O separation, R(Cu–O), was noticed in 1995 by Rao and Ganguli (see inset in Fig. 4).[47] These authors analyzed the properties of 23 oxocuprate SCs and observed that "the highest T_C values occur in the 1.89–1.94 Å range. When R(Cu–O) < 1.88 Å the material is metallic; those with R(Cu–O) > 1.94 Å are certainly insulating" and that the largest T_C values are clustered around R(Cu–O) = 1.92 Å.

The remarkable T_C *vs.* R(Cu–O) relationship was recently re-analyzed for nearly 100 distinct families of oxocuprate SCs known to date (Fig. 4).[48] It turns out that the 'magic' Cu–O separation equals 1.923 Å, and that adopting a structure which exhibits this in-plane Cu–O distance does not guarantee, but may potentially lead to, the largest achievable T_C value at ambient pressure, *i.e.* about 140 K. How external pressure modifies the T_C *vs.* R(Cu–O) relationship (*i.e.*: is there another 'magic' Cu–O distance typical for the high pressure regime, and independent of the type of oxocuprate SC?) is not completely clear because precise numerical data is lacking for the majority of oxocuprates subjected to high pressures. There are, however, important indications that – at least for certain types of SCs – pressure alone without chemical doping may lead to the appearance of superconductivity.[49]

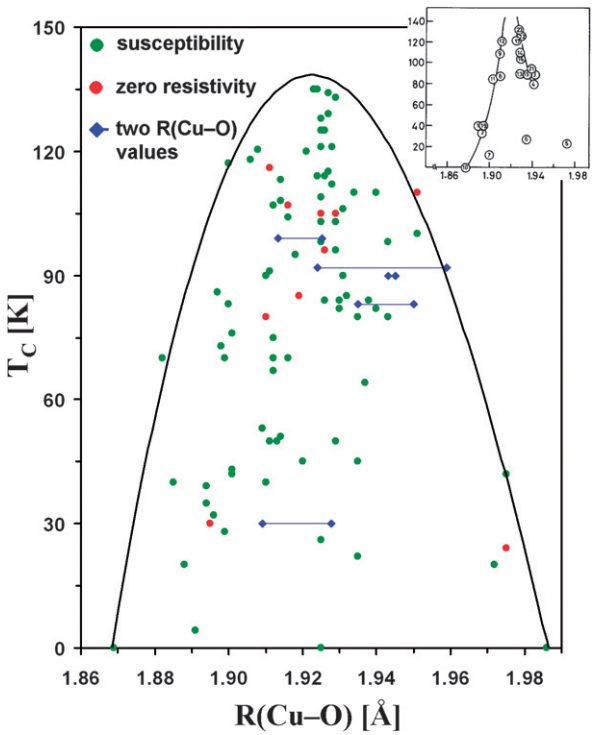

Fig. 4 Illustration of the 'magic' Cu–O bond length of 1.922 Å for about one hundred families of optimally doped oxocuprate SCs. The least-squares fit of the boundary with the 3rd order polynomial is marked with the solid line. The original 1995 plot from ref. 47 is shown in the inset. Reproduced from ref. 48 with permission.

The existence of the 'magic' Cu–O bond length has been rationalized[48] with Burdett's model of superconductivity.[50,51] We now proceed to describe in detail this intuitive chemical approach, since it has served as strong inspiration for the theory-driven quest for superconductivity in fluoride materials.

3.3 Nature of the 'magic electronic state' of oxocuprate SCs

The nature of the superconducting state in oxocuprates has not been fully explained, and is controversial despite over two decades of intense research worldwide. It is, of course, impossible to discuss here all the important scenarios, which have been proposed to account for the large values of T_C in these materials. We choose to concentrate, instead, on a simple real-space model

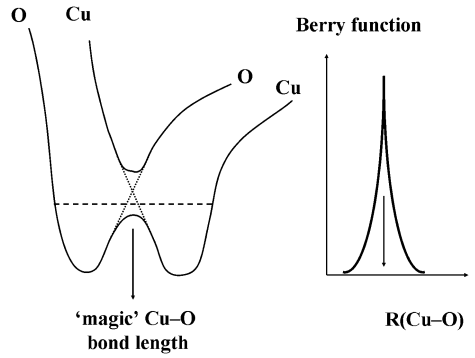

Fig. 5 Illustration of the proposed intersection between Cu- and O-dominated states, which is strongly affected by Cu–O stretching vibrons (- - -), and the Berry function (see text) as a function of R(Cu–O). The left-hand part of the figure is reproduced from ref. 48 with permission.

based on a chemical way of thinking about redox (electron transfer) reactions and their role for superconductivity.

In an insightful 1993 study,[50] further elaborated in 1995,[51] Burdett postulated "without proof" that oxocuprate SCs exhibit an "avoided crossing with interatomic separation of the two energetically close states, one containing electron holes on copper and the other … on oxygen" (see Fig. 5), and – using the notion of a 'critical' Cu–O separation, R_{crit} – he pointed out that "the nature of the electronic state at R_{crit} is very sensitive indeed to changes in interatomic separation". Naturally, it is tempting to associate Rao's 'magic' Cu–O distance with Burdett's R_{crit}, and such a link has recently been made.[48]

The electronic wavefunction of the system, Ψ, may be represented as a linear combination of covalent and ionic contributions:

$$\Psi = c_{cov}\,\varphi_{cov} + c_{ion}\,\varphi_{ion} \quad (5)$$

while the Berry function,[52] (dc_{cov}/dR(Cu–O)) is a convenient measure of changes in the character of the wavefunction as the Cu–O bond length is varied. Here, the covalent Cu-predominated function corresponds to the right-hand side of eqns (1) or (3), while the ionic O-predominated function represents the left-hand side of these equations.

Burdett's model is obviously a rough approximation; it utilizes potential energy curves which are not appropriate descriptions for solids, and in consequence it does not indicate which Cu–O stretching mode of the $[CuO_2]$ sheet is the most important for superconductivity. In fact, several different phonons (notably: breathing, half-breathing, quadrupolar Q_2 and bond buckling) are engaged in substantial coupling, as evidenced by various methods.[53]

Despite its simplicity and limitations, Burdett's model possesses a few key features which persuasively link it with the experimentally observed behaviour of oxocuprate SCs:

1 The model emphasises the need to achieve a subtle equilibrium between the two electronic configurations, and a dramatic change of the electronic wavefunction Ψ with the change of the Cu–O distance in the vicinity of the critical Cu–O separation, *i.e.* the existence of 'a quantum critical point'. Such 'edge-on' behaviour is typical of oxocuprates, which are vulnerable to doping level, external pressure, the presence of impurities within the $[CuO_2]$ layers, and more.

2 The model predicts a substantially non-adiabatic character for oxocuprate SCs ('valence fluctuation'), and a very strong and non-trivial electron–phonon coupling restricted to a very narrow R(Cu–O) range. Specifically, it is possible that all or the majority of the coupling is captured during the vibration (*i.e.* within the vibrational amplitude) which would lead to a very small or even vanishing isotope effect on T_C. This is in agreement with what is seen for many oxocuprate SCs and consistent with the unusual 'peak structure' of the electron–phonon coupling constants in the reciprocal cell noticed recently for various SCs.[54] It also means that to correctly describe the case illustrated in Fig. 5, the modified BCS theory of superconductivity[55] needs to discard the strict assumption of a constant electron–phonon coupling around the Fermi level over a range of $\pm h\omega_D$ (where ω_D is the cut-off Debye frequency). In addition, the inverse isotope effect experimentally observed for PdH_x may be explained by this model.[56]

3 Burdett's model nicely accounts for the fact that superconductivity arises at the metal (overdoped SC; wavefunction dominated by ionic contribution)/insulator (non-doped or underdoped SC; wavefunction dominated by covalent contribution) boundary (Fig. 6).

4 Due to the fact that selected species on the left and right sides of eqns (1) and (3) have a free-radical character ($Cu^{2+\bullet}$, $O^{-\bullet}$), and that the antibonding mixture of the $3d(x^2-y^2)_{Cu}$ and $2p(x,y)_O$ states is responsible for both superconductivity and antiferromagnetism, one may connect Burdett's model with the importance of the strength of the magnetic coupling within the $[CuO_2]$ planes for superconductivity ('spin fluctuations' around the magic R(Cu–O) separation). This means that instead of only discussing electron–phonon coupling one should also consider the influence of lattice distortions on magnetic coupling.[57] One might expect that the size of the intrasheet magnetic superexchange constant J (largely responsible for AFM coupling as quantified by the Néel temperature for the parent non-doped oxocuprate) will be correlated with the intraplane electron–phonon and electron–magnon coupling, and thus proportional to a substantial fraction of the T_C value. Indeed, the large sensitivity of magnetic coupling to deformation of the $[CuO_2]$

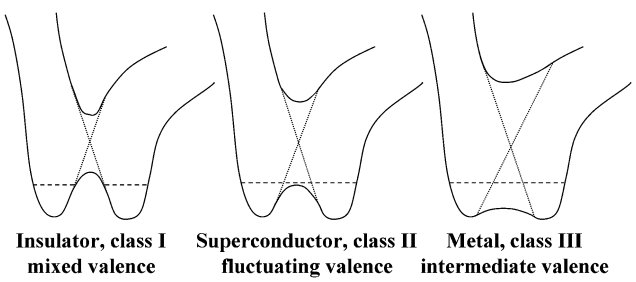

Fig. 6 Illustration of the connection between the appearance of the superconducting state at the insulator (localized electrons)/metal (itinerant electrons) boundary and the historical classification of molecular mixed-valence systems according to Robin and Day, using the theoretical framework of Burdett's model of superconductivity in oxocuprates.[58] The electronic mixing parameter, Δ, gradually increases from left to right, as other parameters are kept constant.

sheet along the breathing mode has been recently demonstrated by LSDA + U calculations for $CaCuO_2$.[48]

Aside from its experimental support, Burdett's model has several features which render it very attractive to chemists:

(A) The model operates in real and not reciprocal space, encouraging chemists to think about superconductivity.

(B) It allows conceptual tuning between insulating, superconducting and metallic states by changing *one* factor: the electronic mixing parameter Δ (see section 4.1) or alternatively the energy of the phonon mode in question. Use of the electronic mixing parameter Δ is important because Δ is related to the degree of covalence of the chemical bond involved in a resistance-free flow of charge.

(C) The model may be overlapped with the historically important classification of the mixed-valence compounds by Robin and Day[58] (Fig. 6) thus offering a nice link between molecular and extended systems.

(D) The model is relatively easy to extend to other systems while utilizing chemical intuition about redox reactions.

Despite these apparent advantages, Burdett's model also yields one important warning:

(E) Since the crossing point of the two electronic states occurs at the typical equilibrium bond length, thus producing a dynamic equilibrium of two electronic states, it will be difficult to reproduce the electronic structure of any high-T_C SC in 'static' quantum mechanical calculations.

Conscious of these difficulties and of the virtues of Burdett's model, let us now learn how to influence the strength of vibronic coupling in small molecules (section 4). These two ingredients taken together will allow us to search for novel families of high-T_C SCs (sections 5 and 6).

4 Influencing the strength of vibronic coupling: a chemist's view

4.1 Dynamic vibronic coupling in triatomic mixed-valence radicals: Marcus-type model

The adiabatic Potential Energy Surface (PES) of any mixed valence system – such as those shown in Fig. 6 – may be modelled with a simplistic Marcus-type approach.[59] The model may be applied to the simplest mixed-valence systems, namely linear triatomic radicals of the ABA type (say, NaFNa). Such systems might be treated as $[A^+ \ldots B^- \ldots A^+]$ cations with one extra electron. The most interesting issue here is whether the molecule preserves its mixed-valence character and stays asymmetric (localization of a supplemental electron), or rather become symmetric and exhibit intermediate valence (delocalization of a supplemental electron, Fig. 7), for example:

$$[Na^+–F^-\cdots\cdots Na^0] \leftrightarrow [Na^{1/2+}\cdots F^-\cdots Na^{1/2+}] \leftrightarrow [Na^0\cdots\cdots F^-–Na^+] \quad (6)$$

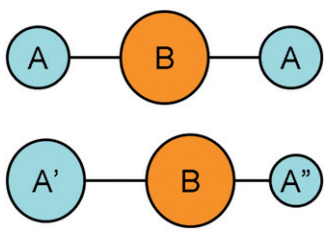

Fig. 7 Linear ABA radicals: symmetric or asymmetric? Intermediate- (A) or mixed-valence (A′, A″)? Compare Fig. 6 and eqn (6).

According to the model proposed, the eigenvalues of the potential energy along the normal nuclear coordinate which desymmetrizes an intermediate-valence system, Q, may be expressed as:

$$E_\pm = \tfrac{1}{2}kQ^2 + (\Delta^2 + V^2Q^2)^{1/2} \quad (7)$$

where Δ [eV] is the electronic coupling parameter, V [eV Å^{-1}] is the vibronic coupling constant, k [eV Å^{-2}] is the force constant for the asymmetric stretch in the hypothetical absence of vibronic coupling, and the '±' index refers to the lower (–) and the upper (+) (excited) PES.

It turns out that the magnitude of Δ, V and k influence the propensity of the ABA system towards asymmetrization. If:

$$V^2 > \Delta k \quad (8)$$

then a symmetric molecule becomes unstable along the Q coordinate and it spontaneously desymmetrizes (system localizes the

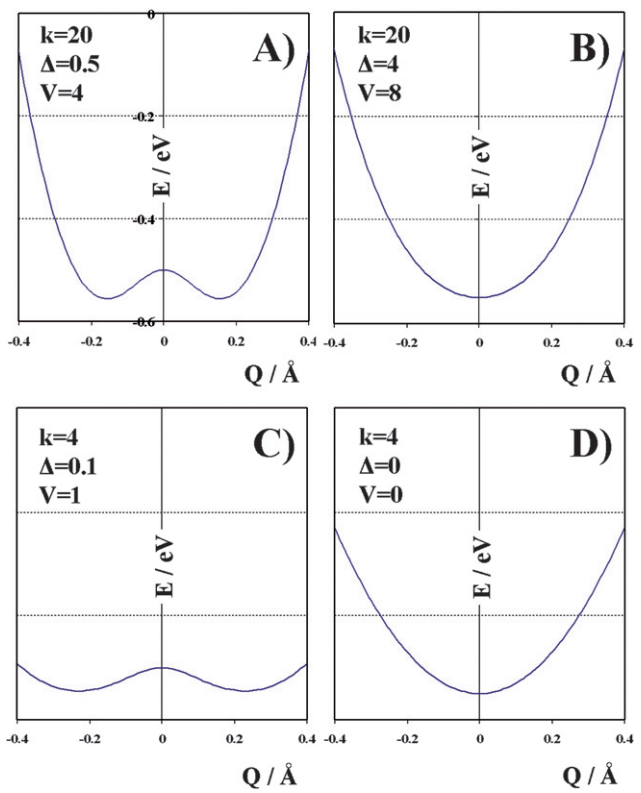

Fig. 8 Influence of the values of k, Δ and V (within the three-parameter model described in the text) on the shape of the ground PES in a mixed-valence system. Four different sets of parameters (A–D) were used for drawing the PES. Note that substantial vibronic coupling, as measured by V, may be hidden in symmetric, nominally intermediate-valence systems (B) and that even weak coupling may reveal itself as an asymmetrizing distortion (C).

appendant electron). In such a case, the lower PES has the character of a well-known double-minimum well, with two equivalent energy minima at:

$$Q^0 = \pm[(V/k)^2 - (\Delta/Q)^2)^{1/2}] \quad (9)$$

If condition (8) is fulfilled, the vibronic coupling is considered to be strong, and if the opposite is true, it is considered weak (the system remains symmetric). It is, however, necessary to emphasize here that substantial vibronic coupling may be hidden even in certain symmetric systems – provided that the Δk product is large enough to keep the molecule in the intermediate valence state (Fig. 8).

The model presented correctly accounts for most experimentally observed features of mixed-valence and intermediate-valence systems (as well as those at the boundary between the two categories, such as the famous Creutz–Taube ion, where localization/delocalization is strongly dependent on the dynamic scale considered), and facilitates understanding of the electron-transfer reactions between two metal centers exhibiting two different valences. Unfortunately, it is not simple to guess what values may be taken by parameters introduced by the model – in particular by V and Δ – in real molecules, and thus the essential questions "Will a molecule remain symmetric?" and "How pronounced is the vibronic coupling?" cannot be answered without knowing Δ, V and k for every particular case. Vibronic instabilities have been therefore calculated for a large set of triatomic radicals using Density Functional Theory (DFT) methods.

4.2 Lessons from triatomic radicals: DFT picture

The DFT screening of a large set of ABA molecules (Fig. 9) preceded by more general considerations of the bond distortions caused by excess electrons or holes and by electronic excitations from the ground singlet to the first excited triplet state has been performed by Grochala and Hoffmann.[60–64] Quantification of the dynamic vibronic coupling constants was subsequently achieved.[65]

These authors have observed that (i) the largest vibronic instabilities occur for the interhalogen ABA compounds including hydrogen halides (A, B = F, Cl, Br, I, H), and (ii) it is particularly large for homonuclear systems (A = B). Indeed, the most pronounced vibronic stability, as measured by the force constant for the imaginary desymmetrizing mode, has been calculated for the F_3 radical (Fig. 9).

To become vibronically unstable, a symmetric ABA radical must (i) consist of strongly electronegative A and B elements (with their Pauling electronegativity not smaller than 2.0), and (ii) exhibit substantially covalent bonds. Result (i) reflects the tendency to localize valence electrons exhibiting large binding energies and occupying contracted atomic orbitals, and helps to rationalize the fact that electronegative O atoms constitute an essential atomic ingredient of high-T_C oxocuprate SCs. An explanation of the importance of substantial covalence of the A–B bonds for large vibronic instability (ii) has been provided by the Molecular Orbital (MO) analysis at the extended Hückel level of the generalized HHH radical where the extended Hückel H_{ii} parameter for the central pseudo-H atom has been varied over a broad energy range (Fig. 10).[63]

It turns out that the strength of vibronic coupling in the three-electron three-orbital model system is *predominantly* governed by the ease with which MOs maximize orbital mixing along the normal coordinate of the asymmetrizing mode, Q, and not by the difference in energy of the mixing orbitals (*i.e.* SOMO − 1 *vs.*

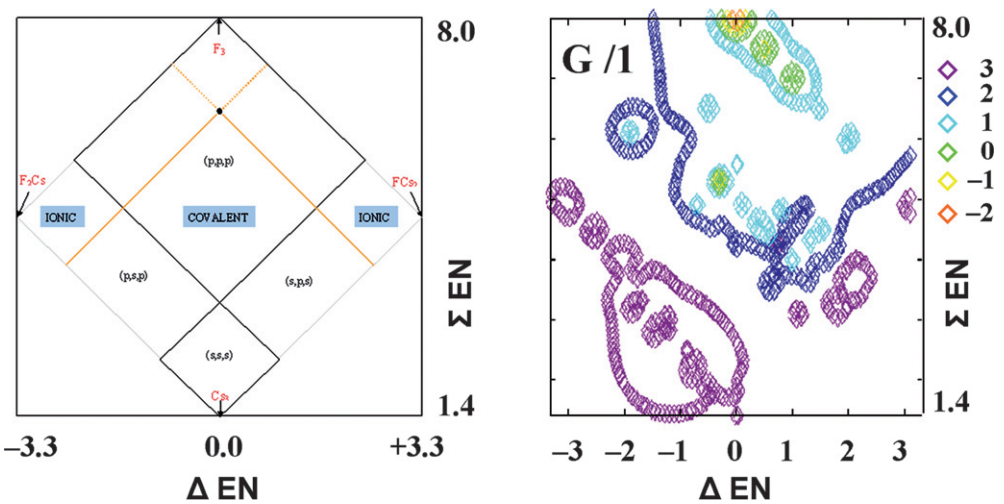

Fig. 9 Illustration of vibronic instabilities in the linear symmetric ABA radicals. Left: Schematic guide-plot for figure on the right. The abscissa is the difference of Pauling electronegativities of A and B elements constituting the A_2B molecule (Δ EN). The ordinate is the sum of Pauling electronegativities of B and A elements (Σ EN). "Ionic" molecules may be found at left and right of the diagram. "Covalent" molecules are found in the middle of the diagram. The labels "ionic" and "covalent" refer not to molecules in a given square, but to a rough region where |Δ EN| is large and small, respectively. Cs_3, F_3, Cs_2F and CsF_2 molecules determine the corners of the diagram. The plot is divided roughly into four areas: "intermetallic" (s,s,s) molecules, "salt-like" (s,p,s) and (p,s,p) molecules and (p,p,p) molecules built of nonmetals. The black dot represents a homonuclear A_3 molecule. Orange solid lines indicate the position of possible A_2B and AB_2 molecules, where A formally serves as an anion. A_2B and AB_2 molecules, where A formally serves as a cation, are found along the orange dotted lines. Right: Map of dimensionless vibronic stability parameter (G) in the periodic table of elements. G is defined as the ratio of the force constants for the asymmetric and symmetric stretching modes. G formally takes a negative value when the asymmetric stretching mode has an imaginary frequency. Reproduced with permission from ref. 63, with changes.

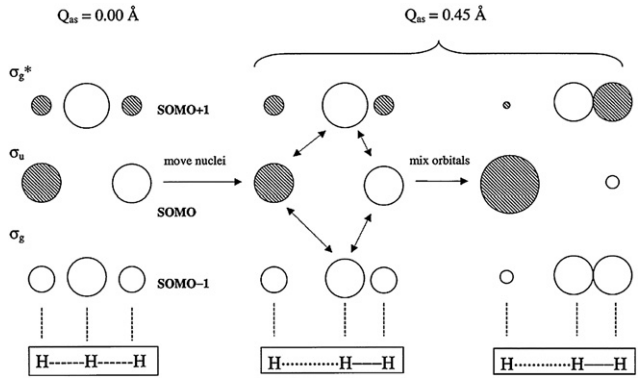

Fig. 10 Illustration to the two-step approach to vibronic coupling for the H_3 radical: step 1 – move nuclei, step 2 – mix MOs. Reproduced with permission from ref. 63.

SOMO, SOMO *vs.* SOMO + 1). In other words, the separation of the orbitals on the energy scale may be large as long as these orbitals may mix efficiently *upon* asymmetrization (Fig. 7). The mixing is most effective when the atomic orbitals of the central pseudo-H and terminal H atoms have the same energy (H_{ii}). This result is important since it helps to rationalize the fact that the largest vibronic instabilities have been previously calculated for the homonuclear triatomic ABA radicals (A = B).[61–63] These conclusions – which may also be extended to one-dimensional solids[66] – have been confirmed in the systematic theoretical studies of Atanasov and Reinen, who studied the vibronic instability of various small molecules along the lone-pair exposing 'umbrella mode'.[67]

In conclusion, the properties of the bridging B atom greatly influence the electron transfer between the two terminal atomic centers A. In the general case, the condition A = B is not required

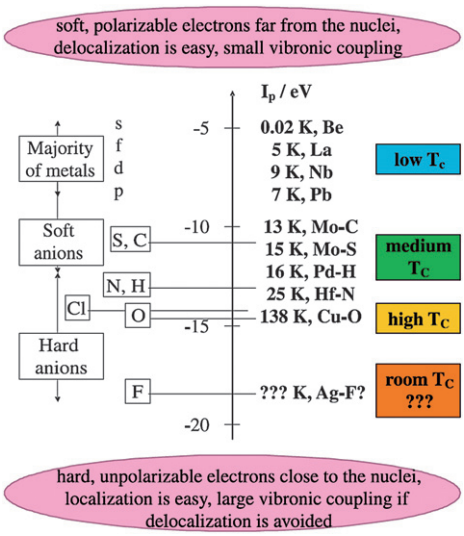

Fig. 11 Various families of inorganic superconductors with their T_C values shown *versus* the first ionization energy (I_P) for the more electronegative of the atoms that form the conducting backbone of each compound. Note that for all superconducting systems shown here, the states at the Fermi level are composed of strongly mixed valence states of cations and anions (substantial 'covalence'). Reproduced with permission from ref. 65.

for achieving strong vibronic coupling in molecules and extended lattices made up from A and B atoms. It is sufficient that A and B possess valence orbitals which can mix very effectively with each other. This is also the case for oxocuprate SCs where the O(2p) set mixes heavily with the Cu(3d) functions.[50,51] A good match of the valence atomic functions of the component elements and the presence of nonmetals or semi-metals is also pre-eminent for other families of SCs such as oxobismuthates, oxoplumbates, nitrides of early transition metals, hydrides, sulfides, carbides (Fig. 11), MgB_2, fullerides, and the recently discovered iron arsenides.[29,33]

4.3 Where to search for large vibronic coupling? A summary

The 'materials aspects' of vibronic coupling[48,60–66] may be summarized as follows:

(1) Large vibronic coupling should be looked for in the connections of the most electronegative elements (*i.e.* nonmetals), in particular those of F and H. Materials based on the most electronegative reactive element – fluorine – might outperform T_C record-holding oxide SCs.

(2) The role of the bridging element X is essential for electron transfer between the bridged atomic centers Y; substantial covalence[68] of the X–Y bonds is crucial for achieving large vibronic instabilities. The presence of an 'avoided crossing' of the electronic PESs of X and Y greatly enhances vibronic coupling in the system. Materials should be investigated where F is *bridging* between two centers, preferably exhibiting mixed valence.

(3) Achieving metallic conductivity for 'hard', unpolarizable valence electrons with a low-lying Fermi level, *i.e.* for very strong nonmetal-based oxidizers, is technically difficult (due to a preference for electron localization) but it may ultimately deliver room-temperature SCs (dynamic intermediate-valence, Fig. 6).

These three prescriptions for high-T_C SCs should be married with the fourth, empirical one:

(4) The highest-T_C SC arises in 2D frameworks at the metal–AFM insulator borderline (see Cu–O and Fe–As connections).

5 The quest for two-dimensional fluorides with substantially covalent element–fluorine bonding

5.1 Fluorides of p-block nonmetals and semi-metals with substantially covalent element–F bonds

Guided only by indications (1) and (2) mentioned above, one would be prone to investigate various interhalogen and hydrogen–halogen connections. Indeed, element–F bonds in such systems must exhibit a substantial degree of covalence.

Let us start with iodine. Unfortunately, the known iodine fluorides (IF, IF_3, IF_5 and IF_7) do not form any genuine mixed-valence phases, which is somewhat surprising for an element which forms as many as four distinct stoichiometric fluorides. The same fate is shared by many other nonmetallic and semi-metallic elements, X, in the p-block: Br and Cl (XF, XF_3, XF_5), S, Se, Te (XF_2, XF_4, XF_6), N (NF_3), P and As (XF_3, XF_5), C and Si (XF_4), and B (BF_3) (Fig. 12). One might possibly attempt to prepare the mixed-valence fluorides of the p-block nonmetals at modest-pressure conditions. Yet large vibronic coupling in hypothetical odd-electron systems of this type (for example, an equimolar mixture of $I(III)F_3$ and $I(V)F_5$) would certainly lead to

13	14	15	16	17
B	C	N	O	F
Al	Si	P	S	Cl
Ga	Ge	As	Se	Br
In	Sn	Sb	Te	I
Tl	Pb	Bi	Po*	At*

Fig. 12 Division of elements from the p-block of the Periodic Table into those which (a) do not form mixed-valence fluoride phases (in red), (b) form mixed-valence fluoride phases (in blue, Bi has been tentatively included in this group). Radioactive elements are marked with an asterisk.

the appearance of genuine mixed-valence species and in consequence the insulating behaviour of such solids if at ambient pressure (see point 3 in section 4.3). Metallization of such solids would certainly require very high external pressures. It is really difficult to imagine that systems of this kind might adopt intermediate valence (here: $I(IV)F_4^{\bullet}$) at ambient pressure/temperature conditions with a concomitant magnetic ordering of unpaired electrons (*cf.* point 4 in section 4.3).

The situation encountered with the fluorides of p-block nonmetals is not unusual and also occurs for the oxide connections of these elements. Indeed, there are not many free radicals for chemical connections of Group 15–18 elements (*e.g.* $ClO_2^{\bullet}$, $ClO_3^{\bullet}$, $NO_2^{\bullet}$, $NO^{\bullet}$, $Xe_2^{+\bullet}$) which are even kinetically stable at ambient conditions, and these species either easily dimerize (NO_2, NO, ClO_3) or they do not form extended metallic networks but crystallize as 0D solids with rather small magnetic superexchange between electronic spins (ClO_2,[69] $Xe_2Sb_2F_{11}$[70]).

Thus, somewhat compromising the degree of covalence of the element–F bonds, we will now turn to the fluorides of the p-block semimetals and metals and those of the transition metals.

5.2 Fluorides of p-block metals MF_n, with substantially covalent metal–F bonds

Many p-block semimetals and metals have substantial affinity to fluorine, and strong fluoride ion acceptors are found in this class (with SbF_5 heading the ranking).

Al, Ga, and In do not form any mixed-valence fluorides in the solid state. On the other hand, four mixed-valence fluorides of Tl have been synthesized in the past (Tl_4F_6, Tl_2F_4, Tl_3F_7 and Tl_3F_5).[71] All these phases are diamagnetic since they show genuine mixed-valence with distinct Tl(III) and Tl(I) crystallographic sites. The same situation persists for the few known mixed-valence fluorides of Ge,[72] Sn[73] and Pb[74] (Ge_7F_{16}, Ge_5F_{12}, Sn_2F_6, Sn_3F_8, Pb_2F_6, Fig. 13). Five distinct mixed valence Sb(V)/Sb(III) fluorides have been synthesized (Sb_4F_{14}, Sb_4F_{15}, Sb_4F_{16}, $Sb_{11}F_{43}$, Sb_7F_{29}).[75] There are direct fluoride bridges between Sb(III) and Sb(V) in some of these compounds, but they are all diamagnetic, colourless or just weakly coloured (thus the intervalence charge transfer electronic transition falls in the UV range), and in consequence insulating. Analogous connections for As and Bi may be anticipated due to the similar properties of

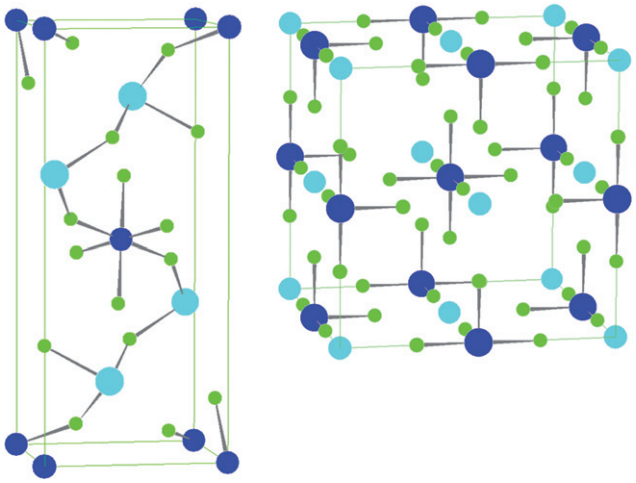

Fig. 13 Crystal structures of two mixed-valence insulating fluorides of tin, Sn_3F_8 (left) and γ-Sn_2F_6 (right) with larger Sn(II) cations in light blue and smaller Sn(IV) in dark blue. Fluoride anions are in green. γ-Sn_2F_6 takes a distorted RuO_3-type structure with six Sn(II)–F bonds at 2.297 Å and six Sn(IV)–F bonds at 1.864 Å. The "SnF_3" lattice differs from the "$AuCl_3$" lattice of mixed-valence $Cs_2Au(I)Au(III)Cl_6$[76] by the way halide anions are distorted from the special (¼ 0 0) positions.

As, Sb and Bi, but they have not yet been explored. It may safely be assumed that these phases would also exhibit mixed valence and not intermediate valence.

To summarize this section, there is little chance indeed for intermediate-valence (*i.e.* genuinely odd-electron) metallic or magnetic fluorides of any p-block semimetal or nonmetal under ambient pressure conditions.

5.3 Fluorides of transition metals with substantially covalent metal–F bonds

Most transition metals (TMs) exhibit very rich chemistry and a broad range of accessible oxidation states. It is therefore advisable to search in this group for metallic metal fluorides with substantially covalent metal–fluorine bonding.

Early TMs, the most electropositive elements in this group, must immediately be discarded since their bonding to F is quite ionic even for the highest available oxidation states (Y^{3+}, Hf^{4+} *etc.*). For example, HfF_4 is a colourless insulating diamagnetic solid, which adopts an ionic crystal structure with all fluoride ligands shared between two Hf(IV) cations (Fig. 14). In addition, low d-electron counts result in occupation of the π^* and not the σ^* orbitals, which usually leads to small vibronic coupling, negligible associated Jahn–Teller distortions and insignificant AFM coupling between electronic spins.

None of the **pentafluorides** or **hexafluorides** of the TMs, despite the marked covalence of the metal–F bonding, are useful for our purposes since they form essentially 0D (*i.e.* molecular) crystals, with isolated $(MF_5)_4$ tetramers or discrete MF_6 molecules, respectively. This is due to the small formal charge of −1 residing on the fluoride anion, the feature which – in contrast to the situation encountered for the isoelectronic oxide anion, O^{2-} – does not permit formation of crystal structures with large dimensionality for metal cations with oxidation states +5 and +6.

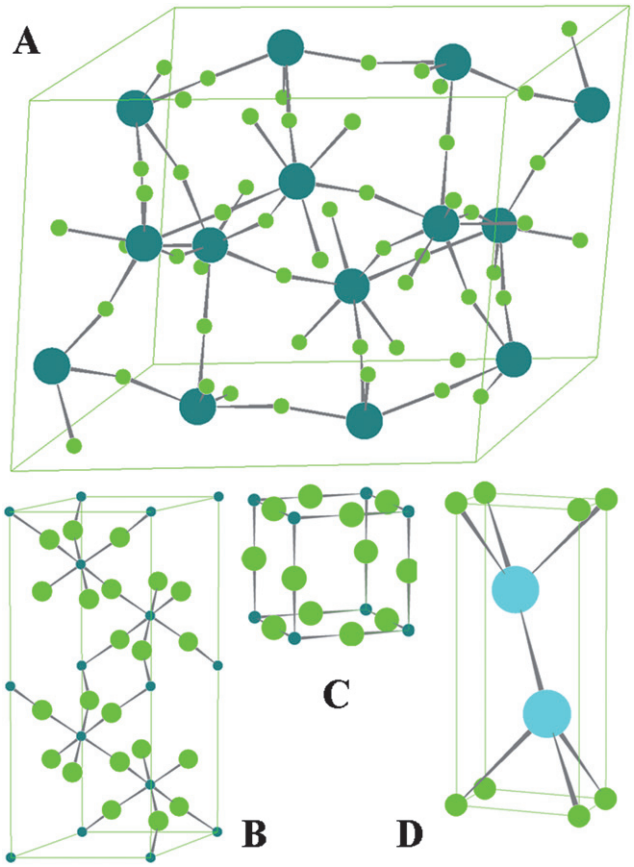

Fig. 14 Unit cells of four different TM fluorides with markedly different magnetic properties and electronic conductivity: A) colourless insulating and diamagnetic $HfF_4 \equiv HfF_{8/2}$ (d^0 electronic configuration); B) violet insulating low-temperature form of $TiF_3 \equiv TiF_{6/2}$, antiferromagnetic below 52 K (d^1), C) metallic and ferromagnetic high-temperature (>370 K) form of TiF_3 (RuO_3 structure) (d^1) and D) bronze metallic Ag_2F, superconducting below 66 mK (anti-CdI_2 structure) (s^{0-1}). Fluoride anions are shown in green.

Obviously, a large magnetic superexchange cannot be expected in the absence of an extended network and most of these materials order magnetically at rather low temperatures of the order of 10 K.[77]

RuF_4 (d^4) is the only layered compound of all the **tetrafluorides** of the late-TMs.[78] However, [RuF_2] layers are strongly puckered while Ru adopts a compressed and not elongated octahedral coordination in this compound. In consequence, the σ* electron does not reside within the [RuF_2] sheets, as required for strong 2D AFM ordering. None of the late-TM tetrafluorides crystallize in the layered structure of the SnF_4-type (NbF_4, with a d^1 configuration, is the only TM fluoride which does[79]).

The majority of TM **trifluorides** crystallize in the trigonal system in the space group $R\bar{3}c$ (Fig. 14)[80] or in various distorted variants of the RuO_3-type structure. Most trifluorides are AFM and the largest Neél temperature (363 K) is seen for a trigonal polymorph of FeF_3.[81] However, this compound owes its large ordering temperature to the large magnetic moment of the high-spin d^5 cation in the weak ligand field rather than to facile superexchange *via* the fluoride bridges; the Fe^{3+}–F^- bonding is quite ionic. Only very few early TM fluorides (NbF_3, TaF_3, MoF_3 and TiF_3 in its high-temperature form, >370 K,[82] Fig. 14) adopt the undistorted RuO_3-type structure. Polymorphism in NiF_3 is rich (with three unpaired electrons at the high-spin Ni(III) centers) and all forms order magnetically below 50 K to *ca.* 200 K.[83] Some polymorphs of NiF_3 and PdF_3 are in fact the mixed-valence M(II)M(IV)F_6 species.[84]

Early TM **difluorides** are very often AFM, similar to trifluorides.[85] The largest Neél temperature (76 K) is seen for the rutile form of FeF_2.[86] This value must be viewed as small since divalent iron has as many as four unpaired 3d electrons in the weak ligand field. TiF_2 constitutes an important exception in this group since this compound crystallizes in the ionic fluorite-type structure, as expected for a quite electropositive TM.[87]

NiF_2, PdF_2 (with atypical high-spin d^8 Pd(II) in both known polymorphic forms[88,89]), CuF_2, and AgF_2 (see Fig. 15) are the only late-TM difluorides known. Among these four important late-TM fluorides only CuF_2 and AgF_2 exhibit layered structures with an elongated octahedral coordination sphere for the TM (Fig. 15), a prerequisite for high-T_C SC. Unfortunately, the [MF_2] sheets are puckered for both compounds. NiF_2 orders AFM only below 74 K,[85] monoclinic CuF_2 below 69 K,[90] but their heavier siblings, PdF_2 and AgF_2,[91] exhibit much larger ordering temperatures. Rutile-type PdF_2 orders FM below 217–225 K[88] while its cubic polymorph is AFM below 180 K.[89] Finally, orthorhombic AgF_2 exhibits FM ordering below 163–165 K.[92] The difluoride of the heaviest element of Group 11, gold, has not yet been synthesized but it seems that AuF_2 would be metastable and exhibit a substantial tendency to disproportionate.

The temperature of magnetic ordering for AgF_2 must be viewed as large, since in contrast to high-spin Pd(II) equipped with two unpaired electrons, Ag(II) has only one unpaired electron per metal center (d^9 electronic configuration). This unusual behaviour of AgF_2 may be traced back to the anomalously large

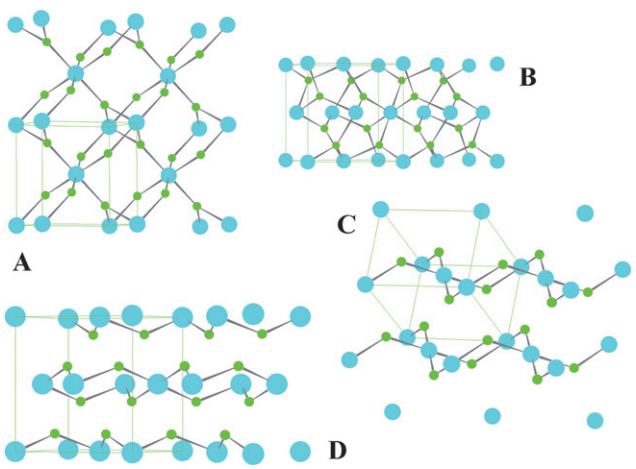

Fig. 15 Crystal structures of four late-TM difluorides with substantial magnetic ordering temperatures: A) rutile PdF_2 (high-spin d^8 electronic configuration), ferromagnetic below 217 K; B) cubic PdF_2, antiferromagnetic below 180 K, C) monoclinic CuF_2 ($3d^9$), antiferromagnetic below 69 K and D) orthorhombic AgF_2 ($4d^9$), ferromagnetic below 163 K. Fluoride anions are shown in green. Note the two-dimensional structures of CuF_2 and AgF_2 with puckered [MF_2] sheets. F atoms – small green spheres.

value of the second ionization potential of Ag, with concomitant substantial covalence of the Ag–F bonds and a large ease of hole (spin) introduction by Ag(II) to the fluoride band (see section 6). All these features render AgF_2 an important precursor for a high-T_C 2D SC.

Very few TM **monofluorides** are known, with ionic AgF as a rare example. High pressure synthesis of metastable AuF from equimolar mixture of Au and AuF_3 has been recently theorized and AuF has been predicted to exhibit 1D [AuF] chains with substantially covalent Au–F bonds and possibly metallic conductivity.[93] However, the 1D structure does not make AuF an attractive precursor for a high-T_C SC.

Only one TM **subfluoride** is known, and that is Ag_2F.[94] Ag_2F shows a 2D crystal structure (Fig. 14), metallic conductivity and even superconductivity below 0.066 K but it owes its metallic character to partial filling of the 5s and not the 4d band. In other words, the silver sublattice is metallic and the atomic orbitals of fluorine almost do not participate in states close to the Fermi level of this interesting compound. Needless to say, appreciable vibronic coupling *via* bridging fluoride anions cannot be expected for this solid.

Summarizing this section we should say that the quest for TM fluorides with substantially covalent metal–fluorine bonding, large magnetic ordering temperatures and quasi-2D crystal structures has led us to *one candidate only*: AgF_2. Our attention has therefore turned to AgF_2 and its derivatives: multinary fluorides of divalent silver.

6 Unusual fluorides of Ag(II)

6.1 General physicochemical characteristics of the fluorides of Ag(II)

Over one hundred fluoride derivatives of divalent silver are known.[95] The vast majority of them have been synthesized by just two groups: one led by Boris Žemva (Lubljana, Slovenia) in cooperation with Neil Bartlett (Berkeley, USA), the other led first by Rudolph Hoppe and then by Berndt G. Müller (Giessen, Germany). Regardless of the stoichiometry and crystal structure adopted, these compounds share similar chemical characteristics: they are extremely moisture-sensitive, liberating oxygen and small quantities of ozone from water (eqn (10)):

$$AgF_2 + \tfrac{1}{2}H_2O \rightarrow AgF + HF + \tfrac{1}{3}\ O_3. \quad (10)$$

The fluorides of Ag(II) are very strong oxidizers indeed. For example, binary AgF_2 vigorously oxidizes chloride anions in ionic chlorides (AgCl, idealized reaction equation: eqn (11)):

$$AgF_2 + AgCl \rightarrow 2\,AgF + \tfrac{1}{2}Cl_2.^{96} \quad (11)$$

and even appreciably covalent chlorides such as $SiCl_4$ (Fig. 16). The inertness of CCl_4 towards AgF_2 is of a purely kinetic nature.[97] However, CBr_4 (idealized reaction equation: eqn (12)) and CI_4 in the solid state (Fig. 16) are easily attacked by AgF_2; the reaction first proceeds slowly at the intergrain boundary, resulting sometimes in an explosion:

$$4\,AgF_2 + CBr_4 \rightarrow 4\,AgF + CF_4 + 2\,Br_2.^{97} \quad (12)$$

At ambient conditions, AgF_2 oxidizes many – even per-fluorinated – organic compounds.[97] AgF_2 fluorinates $P(C_6F_5)_3$ to $PF_2(C_6F_5)_3$, attacks the isothiocyanate functional group, -NCS, yielding Ag_2S, triggers free-radical polymerization of C_6F_5CN and oxidizes higher fluorosulfonic acids ($C_4F_9SO_3H$, $C_8F_{17}SO_3H$) to the corresponding peroxides. Triflic acid (CF_3SO_3H), usually considered to be a redox-inert superacid, is oxidized by AgF_2 at the boiling point. Fluorination of the C_{60} fullerene with AgF_2 at 300 °C leads to $C_{60}F_{44}$ with an impressive 80% yield.[98] Following the Manhattan project, AgF_2 was used by Cady[99] as a catalyst for fluorination of a variety of organic compounds with gaseous F_2, including aromatic hydrocarbons and alcohols (the latter are selectively oxidized to hypofluorites, ROF).

Ag^{2+} is in principle incompatible with oxides and chlorides. At elevated temperature (100–300 °C) AgF_2 attacks all binary chlorides and the majority of binary and ternary oxides in the solid state (with evolution of oxygen).[96] Only selected sulfates, chromates, nitrates, perchlorates, permanganates and perrhenates resist the action of AgF_2 under these conditions.

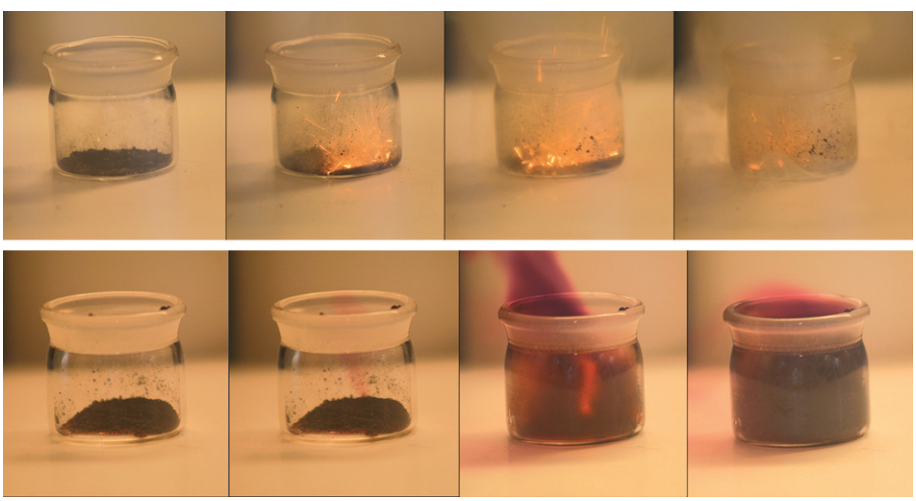

Fig. 16 Vigorous oxidation of $SiCl_4$ (top) and of CI_4 (bottom) by AgF_2. Reproduced with permission from refs. 96 and 97.

When Ag^{2+} salts are dissolved in anhydrous HF made superacidic with the use of SbF_5, the resulting solvated Ag^{2+} cations are capable of oxidizing elemental Xe:[100]

$$2\,Ag^{2+}{}_{solv.HF} + Xe \rightarrow 2\,Ag^{1+}{}_{solv.HF} + Xe^{2+}. \quad (13)$$

The redox reactions expressed by eqns (10)–(13) testify to the great oxidizing power of Ag(II). The standard redox potential E^0 for the Ag(II)/Ag(I) redox pair is +1.98 V in an acidic environment,[10] the corresponding value for the anhydrous HF solution being as positive as +2.27 V.[101] This value exceeds that for the $S_2O_8^{2-}/2SO_4^{2-}$ pair in aqueous solutions, +2.01 V,[102] and it is close to the value for the Xe^{2+}/Xe^0 pair, of +2.32 V in an acidic environment.[10] The E^0 values alone show the enormous differences that exist between the unusual Ag^{2+} and its lighter more common congener, Cu^{2+}; the E^0 value for the Cu(II)/Cu(I) pair is as low as +0.16 V.[10]

The unusually strong oxidizing properties of Ag(II) come from the fact that the second ionization potential of Ag surpasses those of Xe and Se nonmetals, and is the largest of all metallic elements except the alkali metals (Fig. 17).[103]

The inorganic fluorides of chemical elements in their highest oxidation states obviously cannot be oxidized any further, and some of them participate in acid–base reactions involving AgF_2. For example, AgF_2 gradually transfers its F^- anions to a strong Lewis acid:

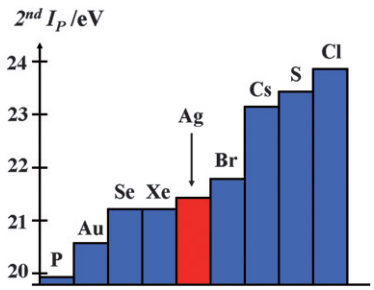

Fig. 17 The values of the second ionization potential for several elements including Ag. Reproduced with permission from ref. 102.

$$AgF_2 + SbF_5 \rightarrow [AgF](SbF_6) \quad (14)$$

$$[AgF](SbF_6) + SbF_5 \rightarrow Ag(SbF_6)_2 \quad (15)$$

or gradually accepts F^- anions from a strong Lewis base:

$$AgF_2 + KF \rightarrow K[AgF_3] \quad (16)$$

$$K[AgF_3] + KF \rightarrow K_2(AgF_4) \quad (17)$$

For Lewis acids and bases of moderate strength reactions (14)–(17) may stop at the first stage, (14) or (16).[95,102]

6.2 The Jahn–Teller effect and plasticity of the coordination sphere of Ag(II)

With nine electrons in its 4d shell, Ag^{2+} is susceptible to the Jahn–Teller (JT) effect, similar to Cu^{2+}. In consequence Ag^{2+} is most often found in either an elongated (normal JT effect) or compressed (inverse JT effect) octahedral coordination (Fig. 18). Other coordination environments are rare. Typical Ag–F bond lengths vary from 2.34 to 2.60 Å (axial, R_{ax}) and from 2.01 to 2.11 Å (equatorial, R_{eq}) for the elongated octahedral site. The corresponding values for the compressed octahedral coordination are 2.00–2.09 Å (R_{ax}) and 2.20–2.42 Å (R_{eq}).[104]

The ellipsoidal Ag^{2+} cation exhibits significant plasticity of its coordination sphere,[105] similar to its lighter d^9 congener, Cu^{2+}: the function of R_{eq} *vs.* R_{ax} is inverse and monotonic (Fig. 18). The Jahn–Teller distortion parameter D ($= R_{ax}/R_{eq}$) takes values from 0.83 to 1.29, with the forbidden range from 0.94 to 1.11 (close to an ideal octahedron).[103] D measures how strongly the $[AgF_6^{4-}]$ octahedron is uniaxially deformed ($O_h \rightarrow D_{4h}$) in real solids.

Obviously, it is the normal JT effect with the associated half-occupation of the $4d(x^2-y^2)_{Ag}/2p(x,y)_F$ hybrid (Fig. 18) which is desired for the appearance of SC in 2D solids. But is the Ag–F bonding covalent enough to result in the large vibronic coupling and crossing of 'ionic' and 'covalent' curves needed to achieve high-T_C SC?

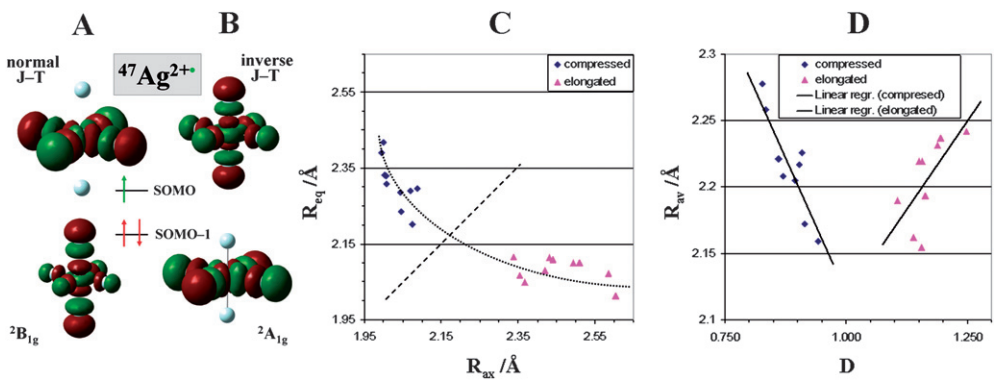

Fig. 18 The Jahn–Teller effect for the Ag^{2+} (d^9 system). The Ag^{2+} cation has a remarkably flexible first coordination sphere and can exhibit either a normal (A) or an inverse JT effect (B). The arrangement of the two uppermost d orbitals in the elongated O_h (4 + 2) ligand field (normal JT effect, left), and in the compressed O_h (2 + 4) ligand field (inverse JT effect, right). Dependence between (C) R_{eq} and R_{ax} Ag–F bond lengths and (D) R_{av} and D for about 20 fluorides of Ag^{2+} (see text). The broken line is drawn in a) for $R_{ax} = R_{eq}$; the dotted line is a guide to the eye. The solid lines in (D) are linear regressions. Reproduced with permission from refs. 102 and 103, after changes.

6.3 Degree of covalence of the Ag–F bonding and ease of magnetic superexchange *via* a bridging F^- anion

Since F is the most electronegative of the reactive elements, one expects metal–fluorine bonds to be quite ionic for connections of metals in low oxidation states, such as 1+ or 2+. This is not the case, however, for electron-hungry Ag^{2+}.

DFT calculations have suggested that the Ag–F bonding is remarkably covalent in all connections of divalent silver.[95] Subsequent core- and valence-X-ray Photoelectron Spectoscopy (XPS) studies have confirmed this interesting result.[106] Using a classical picture of transition metal–ligand bonding, one may divide valence states into (i) metal–ligand bonding ligand-centered states at large binding energies, (ii) nonbonding ligand-centered states at moderate binding energies, and (iii) metal–ligand antibonding metal-centered states at small binding energies. If metal valence orbitals participate substantially in states of type (i) and ligand orbitals in states of type (iii) then the metal–ligand bonding is covalent, when the opposite is true the bonding is ionic. The XPS results for the fluorides of silver at three different valencies (+1, +2, +3) have revealed the following share of $4d_{Ag}$ orbitals to states (i) and (iii): AgF (82%,18%), AgF_2 (58%,42%) and $KAgF_4$ (40%,60%). A nearly 3:2 share for AgF_2 testifies to a marked covalence of the Ag–F bonds in this compound. This feature may be alternatively described as an introduction of holes by Ag^{2+} to the fluoride bands:

$$[Ag^{2+\bullet} + F^-] \leftrightarrow [Ag^{1+} + F^{0\bullet}] \text{ (compare eqn (3).} \qquad (19)$$

Note that AgF_2 is the least thermally stable of all known metal difluorides. Thermal decomposition of AgF_2 is very fast above 690 °C and proceeds according to the equation:

$$AgF_2 \rightarrow AgF + \tfrac{1}{2}F_2 \qquad (20)$$

which shows that at substantially elevated temperature Ag^{2+} is capable of oxidizing fluoride F^- anions; the latter are the least susceptible to oxidation of all known inorganic anions.[107]

Trivalent silver forms even more covalent bonds to fluoride anions. An anomalous exchange of 'metal' and 'ligand' states is seen with XPS (Fig. 19) with a larger share of $4d_{Ag}$ states in the larger-binding energy 'ligand' band than in the smaller-binding energy 'metal' band. This feature may be written as:

$$[Ag^{3+} + F^-] \leftrightarrow [Ag^{2+\bullet} + F^{0\bullet}] \text{ (compare eqn (1).} \qquad (21)$$

The substantial covalence of the Ag–F bonds is one unusual feature of fluoroargentates(II), which makes them similar to oxocuprates(II).

The marked covalence of the Ag–F bonds helps to explain why quite efficient magnetic superexchange is observed between two paramagnetic Ag^{2+} metal centers linked by a fluoride bridge(s) in various compounds (see the large Curie temperature of AgF_2, section 5.3).[95,108] Indeed, DFT calculations for the model system where two $FAg^{2+}(FH)_2$ units have been linked through a single F^- anion[109] (Fig. 20) show that spin polarization of the frontier MOs is substantial for the triplet ground state. The SOMO of this complex (σ*) is Ag–F antibonding for all Ag–F interactions and it consists of two AFM coupled $4d(x^2-y^2)_{Ag}$ orbitals with a substantial share from 2p(x,y)F orbitals. It is remarkable that substantial AFM coupling is observed even for π* orbitals despite the fact that the fluoride anion, found in the middle of the spectrochemical ligand series, is usually considered to be a very weak π-donor and null π-acceptor.[110]

The spin polarization induces a very large separation of α (spin-up) and β (spin-down) states of nearly 3 eV (see the SOMO(α)/SOMO + 1(β) gap in Fig. 20) which testifies to a large magnetic superexchange constant. Unusually strong magnetic interactions are possible because of the substantial mixing of the Ag and F valence orbitals ('covalence').

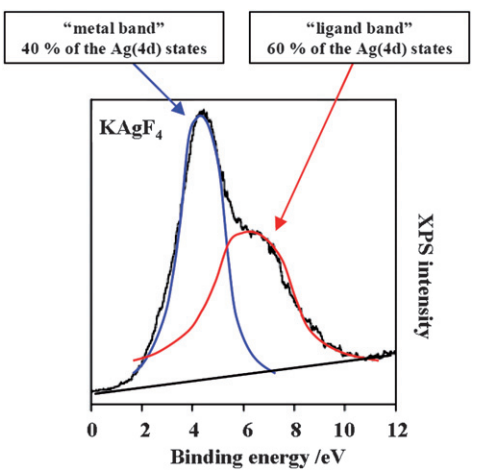

Fig. 19 The valence XPS spectrum of $KAgF_4$, a ternary fluoride of trivalent silver. For discussion see text. Reproduced with permission from ref. 105, with minor changes.

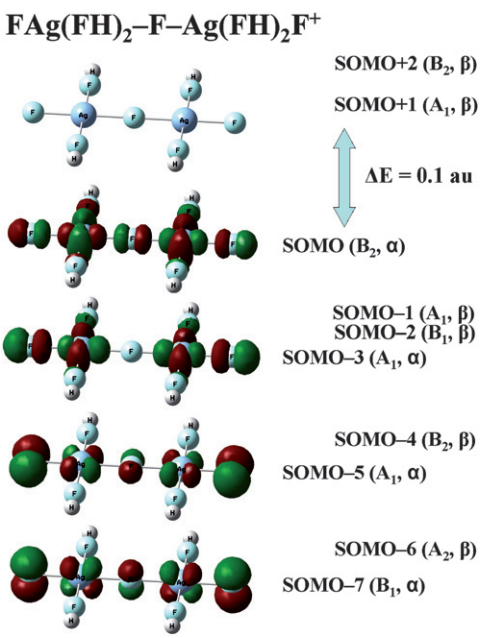

Fig. 20 Selected Kohn–Sham α orbitals of the lowest-lying triplet state of a molecular cation composed of two $FAg^{2+}(FH)_2$ units bridged by a single F^- anion.[109] Note the substantial mixing of $4d_{Ag}$ and $2p_F$ atomic orbitals in both σ* and π* states, as well as an AFM coupling of 4d functions of Ag.

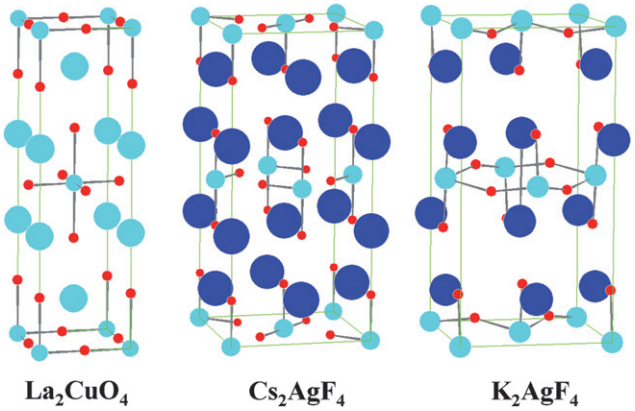

Fig. 21 Comparison of crystal structures for tetragonal La_2CuO_4, and orthorhombic Cs_2AgF_4, and K_2AgF_4. The local coordination sphere of the TM cation takes the form of an elongated octahedron for the first two compounds and of a compressed octahedron for K_2AgF_4. Cu, Ag – small light blue spheres, La –large light blue spheres, K, Cs – large dark blue spheres, O, F – small red spheres.

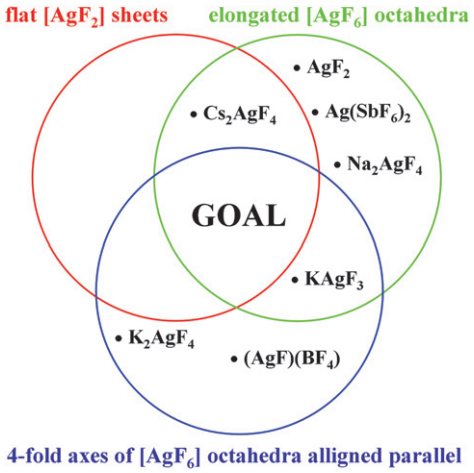

Fig. 22 Division of fluoroargentates(II) into three, sometimes overlapping, sets of compounds: (I) exhibiting flat $[AgF_2]$ sheets, (II) containing elongated $[AgF_6]$ octahedra, and (III) having the long axes of the octahedra aligned parallel to one another. The goal material *i.e.* a layered AFM fluoroargentate(II) (*i.e.* a superconductor precursor) must possess all three features simultaneously (see text).

6.4 Crystal structures and magnetic properties of layered fluorides of Ag(II)

Crystalline fluoroargentates(II) adopt many structure types, with isolated $[AgF_6]$ octahedra, $[AgF^+]$ infinite chains or $[AgF_2]$ sheets as principal structural leitmotifs.[95] The last type is exemplified by binary AgF_2 (Fig. 15D) as well as by the layered $MAgF_3$ and M_2AgF_4 ternaries where M = K, Rb, Cs (Fig. 21), are of most interest for the generation of 2D SC.

Cs_2AgF_4[111] crystallizes quasi-tetragonally, with a marginal difference (~0.004 Å) between two short unit cell vectors (*ca.* 6.48 Å). However, the unit cell cannot be reduced to tetragonal due to the pronounced departure of F atoms within the $[AgF_2]$ sheets from special (¼ ¼ z) positions. Isolated nearly square-planar $[AgF_4^{2-}]$ units (2 × 2.09 Å, 2 × 2.11 Å) stacked perpendicular to one another may be distinguished in the crystal structure. Orthorhombic distortion is much more pronounced for K_2AgF_4[112] (6.18 Å *vs.* 6.44 Å). The ligand environment of Ag^{2+} is now in the form of a compressed $[AgF_2F_{4/2}^{2-}]$ octahedron (2 × 2.08 Å, 4 × 2.26 Å); minor tilting of the octahedra is observed, making the $[AgF_2]$ sheets slightly puckered.

It turns out that the seemingly small distortions of the crystal lattice seen for layered M_2AgF_4 fluoroargentates induce FM ordering[113] and make these compounds magnetically dissimilar to AFM La_2CuO_4 (an important precursor of an oxocuprate SC). Fluoroargentates of Cs and K order FM at 14 K[111,114] and 26 K,[112] respectively, while La_2CuO_4 becomes AFM below 317–325 K.[115] The presence of long Ag–F separations within the $[AgF_2]$ sheets (2.26 Å for the K compound, 2.49 Å for Cs) is to be blamed for the disruption of intra-sheet magnetic communication between the paramagnetic Ag^{2+} centers, and in consequence for the small values of ordering temperatures for these materials. The FM ground state and magnetic moments for Cs_2AgF_4[116,117] and K_2AgF_4[112] have been correctly reproduced by DFT and LSDA+U calculations.

To achieve AFM ordering at an appreciable temperature (100–300 K) a layered fluoroargentate(II) must *simultaneously* exhibit three important features typical of the La_2CuO_4 structure: (i) it must contain elongated and not compressed $[AgF_6]$ octahedra, (ii) the long axes of these octahedra must be aligned parallel and not perpendicular to one another, and (iii) it must exhibit flat and not puckered $[AgF_2]$ sheets (Fig. 22). It is currently unclear how such a structure might be achieved by various chemical substitutions.

6.5 Electronic conductivity and possible superconductivity of fluoroargentates(II)

The majority of fluoroargentates, such as Cs_2AgF_4 and K_2AgF_4 are coloured (blue or violet), they exhibit a substantial band gap (~2 eV) at the Fermi level and they are electrical insulators. However, those fluoroargentates which contain the 1D $[AgF^+]$ chains (usually brown-coloured) exhibit a metallic lustre and Pauli paramagnetism, typical of metallic conductivity.[118] Unfortunately, all attempts to measure the electric conductivity of these compounds with contact methods have failed. The reason for this is the reactivity: even gold wires attached to the samples of the fluoroargentates may be oxidized on their surface, preventing the resistivity measurement.[119] Thus, the non-contact microwave cavity perturbation method has been used to determine the ac-dielectric response of AgF_2 and of $KAgF_3$.[120]

It turns out that brown AgF_2 is an insulator at room temperature and its electric resistivity slightly increases below the Curie point.[120] On the other hand, $KAgF_3$, which exhibits infinite bent 1D $[AgF^+]$ chains,[112] is metallic at room temperature but becomes insulating below the Neél point (68 K).[120] This feature suggests that the electrons responsible for the magnetic ordering of $KAgF_3$ become intinerant above the ordering temperature. The metallic conductivity of $KAgF_3$ has been explained by DFT and LSDA+U calculations.[120,121]

The experimental search for a SC in the fluoroargentates(II) has not been very extensive to date. One result is of particular interest: in 2004 observations were reported of sudden drops in the magnetic susceptibility of a large number of samples in the

BeF_2/AgF_2 system, over temperatures ranging from 8.5 K to 64 K.[122] These magnetic anomalies, strongly reminiscent of the Meissner–Ochsenfeld effect, suggested the presence of superconductivity in a small sample fraction of the Be–Ag–F system (with a possible small O content). The samples studied did not contain any appreciable copper impurities as determined by the ICP MAS method. Thus, traces of oxocuprate SCs could not be responsible for the observed drops in magnetic susceptibility. The true origin of these magnetic anomalies, the possibly superconducting nature of the samples and the identification of the minority responsible for the anomalous magnetic response, still await confirmation.

6.6 Effect of external pressure on structure and properties of binary AgF_2: theoretical predictions

External pressure is an important physical parameter affecting the structure and properties of elements and compounds.[123] Modifications of the crystal structure may be vast, especially as the range of static pressures achievable in the laboratory now extends well over several megabars (1 Mbar = 10^6 atm = 100 GPa). Indeed, external pressure as small as 2.7 GPa induces a phase transormation of AgF from a NaCl- to a CsCl-type structure; an intermediate anti-NiAs structure has also been observed upon subsequent decompression.[124] However, none of the fluoroargentates(II) have so far been subject to experimental high-pressure research.

Theoretical results obtained with DFT methods suggest that the simplest fluoroargentate(II), binary AgF_2 (for crystal structure see Fig. 15), should undergo a phase transition at ~15 GPa to the infinite-layer *Cmca* (δ) structure (Fig. 23).[125] The δ polymorph is characterized by flat [AgF_2] sheets and only slightly bent Ag–F–Ag bridges, thus favouring an AFM superexchange. Indeed, subsequent spin-polarized DFT calculations have predicted that δ-AgF_2 should exhibit an extremely large AFM superexchange constant of −298 meV, a reduced magnetic moment of ~0.2 μ_B on the silver atom, and that this form should transform into a 2D metal or possibly a SC with more pronounced compression (at ~38 GPa).[117]

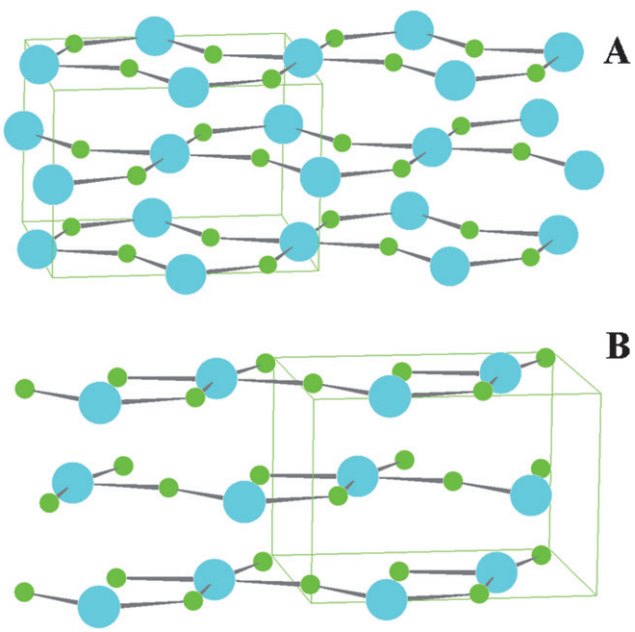

Fig. 23 Illustration of the crystal structures of two possible orthorhombic polymorphs of AgF_2 at 40 GPa, as predicted by DFT methods. A) δ-AgF_2[125] and B) θ-AgF_2.[126] Note the flat [AgF_2] sheets and slightly bent Ag–F–Ag bridges in both structures. Ag – large blue, F – small green spheres.

Phonon calculations suggest, however, that δ-AgF_2 shows two soft phonon branches at 40 GPa; this form might thus be unstable and transform to another closely related orthorhombic ($Cmc2_1$) θ-AgF_2 polymorph (Fig. 22).[126] The calculated difference of electronic energies between the δ and θ polymorphs is in fact very small, *ca.* 25 meV per FU at 40 GPa. The in-plane magnetic superexchange constant of θ-AgF_2 reaches −242 meV at 0 GPa and the this form is metallic at 40 GPa, similarly to δ-AgF_2.

These interesting theoretical predictions now beg for experimental verification. But for this, technical problems must first be overcome related to the aggressive chemical behaviour of AgF_2 with respect to surfaces of diamond and conventional gasket materials (W, Au, BN *etc.*) used in diamond anvil cells.

6.7 Ag(II) linked to non-fluoride-based inorganic anions

As described in previous sections, crystal engineering of fluoroargentates(II) to target a 2D AFM insulator is not straightforward, and it is unclear which chemical substitutions within the known Ag^{2+}/F^- phases might lead to a desired structure. We are therefore tempted to enlarge the field of possibilities by including other inorganic anionic ligands, L, and targeting various Ag–F–L, M–Ag–F–L (M = metal cation) or Ag–L connections. But which inorganic anions might take the place – without being oxidized – in the first coordination sphere of potent Ag^{2+} oxidizer?

Plain oxide (O^{2-}) and chloride (Cl^-) anions must be excluded since their presence leads either to disproportionation of Ag(II) to Ag(I) and Ag(III) – as seen for both the tetragonal and monoclinic forms of $AgAgO_2$[127] – or to an irreversible oxidation of the anion.[96,97,103,128] Fluorosulfate(VI) (SO_3F^-) and triflate ($SO_3CF_3^-$) are the sole oxo-anions which form pseudobinary AgL_2 compounds with Ag(II).[129] It appears, however, that these solids are thermodynamically unstable at ambient conditions.[130] For example, $Ag(SO_3CF_3)_2$ decomposes slowly at room temperature, evolving the peroxo dimer $(SO_3CF_3)_2$.

Recent theoretical[131] and experimental[96] studies suggest that the room-temperature chemistry of Ag(II) might be extended beyond the known fluoride, fluorosulfate and triflate connections, to include perchlorate (ClO_4^-), nitrate(V) (NO_3^-), metaphosphate (PO_3^-), perfluoro-*tert*-butoxo ($^-OC(CF_3)_3$), and possibly even sulfate (SO_4^{-2}) or hydrogensulfate (HSO_4^-). Use of selected anions from this list might enable formation of the pseudoternary Ag–F–L or or pseudoquaternary M–Ag–F–L compounds with the desired structural and electronic features of the [AgF_2] sublattice.

6.8 Organic–inorganic hybrids containing Ag(II)

A large family of connections of divalent Ag with organic Lewis bases is known.[132] Ag(II) binds to the lone pair of a covalently

bound N, as seen in various complexes of Ag^{2+} with pyridine, pyrazine, α,α′-bipirydyl or tripirydyl[133] and with permethylated cyclam.[134] Compounds with Ag–N and Ag–O bonds have also been synthesized as exemplified by complexes of Ag(II) with 2-carboxypirydyl acid and the anion of nicotinic acid. Strong complexation allows for reduction of the standard redox potential for the Ag(II)/Ag(I) pair down to 1.453 V,[132] so synthesis may be performed even in aqueous solutions, using $K_2S_2O_8$, PbO_2, CeO_2 or BaO_2 as oxidizers.[135] It must, however, be realized, that in all cases the synthetic approach towards the N→Ag(II) compounds has relied on the initial ligation of Ag(I) by the N-bases and the subsequent oxidation of Ag(I) to Ag(II). The inverse tactic (first oxidation, then ligation) should prove ineffective because Ag(II) easily fluorinates the C–H bonds present in the organic amines.

The unusual Ag(II)–C bonds exist in several porphyrin derivatives.[136] Two compounds with Ag(II)–S bonds have been synthesized so far and they are thermodynamically unstable.[137]

The vast majority of the above-mentioned Ag–X compounds (X = N, O, C, S) consist of chelating ligands and thus they exhibit a 0D (or at best 1D) character in terms of their electronic and magnetic structure. Pyrazine complexes of Ag(II), for example $Ag(pyrazine)_2S_2O_8$, constitute one remarkable exception; they have not been characterized structurally but they are presumably quasi-2D, like the analogous Cu(II) complexes (Fig. 24A),[138] and they exhibit AFM ordering.[139] These interesting systems are certainly worth revisiting, despite a relatively weak magnetic superexchange expected to take place *via* a long N–C_2–C_2–N skeleton.

It is interesting that, except for isolated $Ag(NCR)_4^{2+}$ cations (R = CH_3, CH=CH_2) in the gas phase,[140] neutral complexes of Ag(II) with various nitriles have not been reported so far. Our own theoretical results indicate that such complexes might be formed, and that the chemistry of Ag(II) might be extended with little effort beyond the known aza connections, to include perfluorinated nitriles and perfluorinated amines.[141] Importantly, complexes of AgF_2 with nitriles or dinitriles might exhibit genuine 2D electronic character with flat [AgF_2] sheets and an elongated O_h coordination of Ag[142] (Fig. 24B).

AgF_2–organic hybrids would be similar to the well-known layered uranium and thorium fluorides (UFO[143] and TFO[144]), where protonated amines serve as a structure-directing reagent. Preparation of such layered compounds will be limited by the ability of the nitrile ligand to withstand oxidation;[145] recollect that AgF_2 is the most strongly oxidizing of all known metal difluorides.[98] The use of perfluorinated ligands does not offer a solution to this problem because of their negligibly small ligating ability.[97]

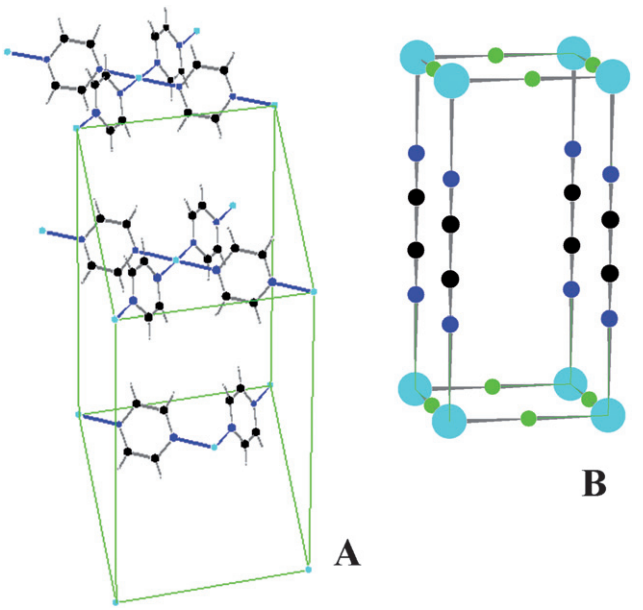

Fig. 24 A) Illustration of the crystal structure of layered Cu(II) $(pyrazine)_2(ClO_4)_2$ complex.[138] Cu – light blue, N – blue, C – black, H – gray spheres. ClO_4 groups have been omitted for clarity. B) Illustration of a hypothetical AgF_2/organic hybrid compound with flat [AgF_2] sheets and elongated O_h coordination of Ag(II) as exemplified by AgF_2/nitrile (here: dicyan, NCCN) 1:1 adduct. Ag – light blue, F – green, N – blue, C – black spheres. Reproduced with permission from ref. 142, with small changes.

6.9 Similarities and differences between oxides of Cu(II) and fluorides of Ag(II)

Combined theoretical and experimental research, partly described in sections 6.1–6.8, permit us to gather evidence for remarkable analogies between fluoroargentates(II) and oxocuprates(II) (*i.e.* precursors of high-T_C SCs).[95] The following similarities have been noticed:

(1) Ag(II) and Cu(II) are isoelectronic (d^9) species, as are F^- and O^{2-} (s^2p^6) species; fluoride and oxide anions are both weak-field ligands.

(2) There is a strong covalent contribution in Ag(II)–F^- bonding (marked covalence), as first indicated by DFT calculations[95] and confirmed by XPS experiments.[106] This makes fluoroargentates(II) very similar to oxocuprates(II). This analogy is additionally supported by similar differences in optical electronegativities[146] between Cu and O and between Ag and F (Δ = 0.8–1.1), which points to comparable ionicity/covalency of the Cu–O and Ag–F bonds in these compounds.[95]

(3) There is a good match between the valence 4d and 2p orbitals of Ag(II) and F, respectively, and those of Cu(II) and O,[147] but Ag(III) is capable of introducing holes into the fluoride 2p band, similar to Cu(III) in an oxide environment.

(4) Electronic structures of isostructural fluoroargentates(II) and oxocuprate (II) are very similar to each other (compare for example a non-spin-polarized electronic structure of idealized (tetragonal) AgF_2 and that of $CaCuO_2$, Fig. 25).[148]

(5) There are apparent crystal structure analogies for both families of compounds. Ag(II) and Cu(II) are both susceptible to the JT effect and exhibit substantial plasticity of their first coordination sphere.

(6) Pronounced AFM magnetic superexchange takes place in undoped flat-sheet [CuO_2] compounds (parent compounds of high-T_C SCs); a similarly large AFM superexchange has been predicted for flat-sheet [AgF_2] species.[117]

However, there are also some important differences between oxides of Cu(II) and fluorides of Ag(II):

(1) Ag(II) and Cu(II) in their respective ligand environments often show qualitatively different JT effects; the coordination sphere of Ag(II) very often takes the form of a compressed

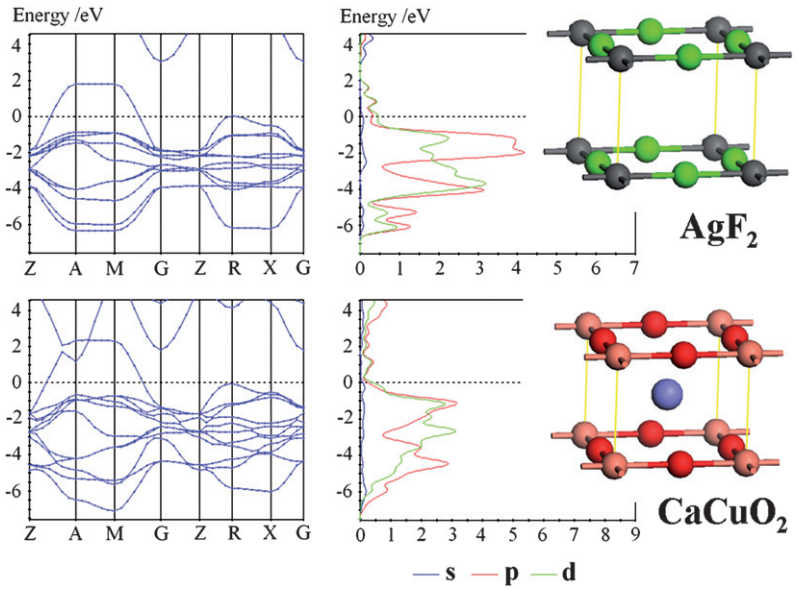

Fig. 25 The calculated non-spin-polarized electronic band structure (left) and partial electronic density of states (right) for hypothetical tetragonal flat-sheet polymorph of AgF_2 and for $CaCuO_2$. Reproduced with permission from ref. 148, after changes.

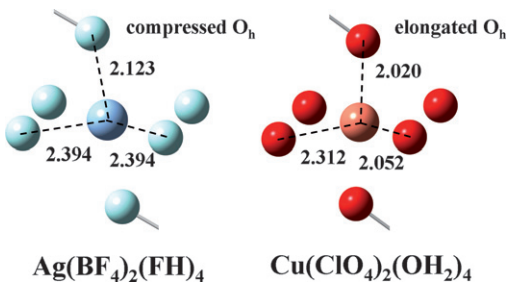

Fig. 26 Comparison of the DFT-optimized equilibrium geometries of $Ag(BF_4)_2(FH)_4$ and quasi-isostructural $Cu(ClO_4)_2(OH_2)_4$ complexes in the gas phase. The coordination sphere of Ag is a compressed O_h (2 + 4), while that of Cu is of the (2 + 2 + 2) type but not far from an elongated O_h (4 + 2). H atoms have been omitted for clarity.[149]

O_h (inverse JT effect, Fig. 26); a similar situation is only rarely encountered for oxa-connections of Cu(II).[149]

(2) There are apparently small distortions in the crystal structure of layered fluoroargentates(II) which facilitate FM and not AFM ordering in these compounds. This is never the case for layered oxocuprates(II). The difference comes in part from charge balance for $[CuO_2^{2-}]$ and $[AgF_2]$ sheets; the latter are much more acidic than the former, and bonds from Ag(II) to apical F atoms are usually short.

(3) Cu(II) oxides do not show a tendency to disproportionate;[150] AgF_2, however, is known in its high-temperature Ag(I)/Ag(III) form).[76,119] The tendency of Ag(II) for disproportionation is even more pronounced in an oxide environment, as exemplified by the lowest-energy $Ag(I)Ag(III)O_2$ polymorph.

(4) Hole- or electron-doping to fluoroargentates(II) often leads to localization of defects (as Ag(III) and Ag(I), respectively) and in consequence to insulating behaviour, as exemplified by several known mixed valence fluorides of silver.[95] Charge localization is extremely seldom observed during doping of layered oxocuprates(II).

Conclusions

In this contribution we have reviewed recent vigorous theoretical and experimental efforts which target an electronically two-dimensional antiferromagnet containing a substantially covalent metal/fluoride sublattice. Particular attention is paid to unusual fluorides of divalent silver. These – so far hypothetical – compounds would be analogous to undoped layered oxides of copper(II), which in turn constitute parent compounds of oxocuprate high-T_C superconductors.

Oxocuprates(II) and fluoroargentates(II) exhibit many remarkable analogies, yet there are also some important differences (see section 6.9). The possibility of reproducing the unique electronic structure seen for oxocuprates(II) and synthesizing the first fluoroargentate superconductor relies largely on the ability to overcome the aforementioned differences between two unique families of compounds.

Note added in proof

While this work was in proof, a careful study of magnetism of a pyrazine complex of Ag(II), described here in section 6.8, appeared.[151]

Acknowledgements

The author acknowledges financial support from ICM and the Faculty of Chemistry (University of Warsaw), from a national KBN grant (N204 167 32/4321) and from the TEAM program of the Foundation for Polish Science. Valuable discussions with Viktor V. Struzhkin (Carnegie Institute, USA), Zoran Mazej (Jožef Stefan Institute, Slovenia), Piotr Leszczyński (Univ. of Warsaw, Poland) and continuing encouragement from Roald Hoffmann (Cornell Univ., USA) are very much appreciated. The critical comments of Andrew J. Churchard (Univ. of Warsaw, Poland) have greatly helped to improve this work. The author is

very grateful to Karol Fijalkowski, MSc, for the concept of the journal back cover, as well as to Andrew J. Churchard and T. Jaron, for their technical assistance.

References

1 N. Bartlett, *Proc. Chem. Soc. (London)*, 1962, 218.
2 L. Khriachtchev, M. Pettersson, N. Runeberg, J. Lundell and M. Räsänen, *Nature*, 2000, **406**, 874.
3 See also recent prediction of the first metastable neutral molecules containing chemically bound helium, $M^+[OHeF^-]$ where M = Cs, NMe_4: W. Grochala, *Polish J. Chem.*, 2009, **83**, 87.
4 M. Kaupp and H. G. von Schnering, *Angew. Chem., Int. Ed. Engl.*, 1993, **32**, 861; X. Wang, L. Andrews, S. Riedel and M. Kaupp, *Angew. Chem.*, 2007, **119**, 8523.
5 S. Riedel and M. Kaupp, *Angew. Chem., Int. Ed.*, 2006, **45**, 3708.
6 H. D. B. Jenkins, H. K. Roobottom and J. Passmore, *Inorg. Chem.*, 2003, **42**, 2886.
7 Report on protonation of HSO_3CF_3 acid by HF/SbF_5: A. Kornath, R. Seelbinder, N. Götz, R. Minkwitz, and R. Ludwig, *15th European Symposium on Fluorine Chemistry*, 15–20 July 2007, Prague.
8 B. Žemva, K. Lutar, A. Jesih, W. J. Casteel, Jr., A. P. Wilkinson, D. E. Cox, R. B. Von Dreele, H. Borrmann and N. Bartlett, *J. Am. Chem. Soc.*, 1991, **113**, 4192.
9 S. Seidel and K. Seppelt, *Science*, 2000, **290**, 117.
10 Values taken from www.webelements.com, accessed on December 30, 2008.
11 W. Grochala, unpublished data.
12 H. K. Ohnes, Commun. Phys. Lab. Univ. Leiden, 1911, 122b and 124b.
13 H. K. Ohnes (1913), L. D. Landau (1964), J. Bardeen, L. N. Cooper and R. Schrieffer (1972), L. Esaki, I. Giaever and B. D. Josephson (1973), P. L. Kapitsa (1978), J. G. Bednorz and K. A. Müller (1987), A. A. Abrikosov, V. L. Ginzburg and A. J. Leggett (2003); from nobelprize.org.
14 W. Meissner and R. Ochsenfeld, *Naturwissenschaften*, 1933, **21**, 787.
15 Z. K. Tang, L. Zhang, N. Wang, X. X. Zhang, G. H. Wen, G. D. Li, J. N. Wang, C. T. Chan and P. Sheng, *Science*, 2001, **292**, 2462.
16 S. Yamanaka, E. Enishi, H. Fukuoka and M. Yasukawa, *Inorg. Chem.*, 2000, **39**, 56.
17 J. H. Tapp1, Z. Tang, B. Lv, K. Sasmal, B. Lorenz, P. C. W. Chu and A. M. Guloy, arXiv:0807.2274, 2008.
18 J. L. Sarrao, L. A. Morales, J. D. Thompson, B. L. Scott, G. R. Stewart, F. Wastin, J. Rebizant, P. Boulet, E. Colineau and G. H. Lander, *Nature*, 2002, **420**, 297; N. J. Curro, T. Caldwell, E. D. Bauer, L. A. Morales, M. J. Graf, Y. Bang, A. V. Balatsky, J. D. Thompson and J. L. Sarrao, *Nature*, 2005, **434**, 622.
19 R. J. Cava, H. Takagi, B. Batlogg, H. W. Zandbergen, J. J. Krajewski, W. F. Peck, R. B. Vandover, R. J. Felder, T. Siegrist, K. Mizuhashi, J. O. Lee, H. Eisaki, S. A. Carter and S. Uchida, *Nature*, 1994, **367**, 146.
20 M. I. Eremets, V. V. Struzhkin, H.-k. Mao and R. J. Hemley, *Science*, 2001, **293**, 272.
21 S. Kometani, M. Eremets, K. Shimizu, M. Kobayashi and K. Amaya, *J. Phys. Soc. Jpn.*, 1997, **66**, 2564; V. V. Struzhkin, R. J. Hemley, H. K. Mao and Yu. A. Timofeev, *Nature*, 1997, **390**, 382.
22 M. I. Eremets, I. A. Trojan, S. A. Medvedev, J. S. Tse and Y. Yao, *Science*, 2008, **319**, 1506.
23 M. I. Eremets, K. Shimizu, T. C. Kobayashi and K. Amaya, *Science*, 1998, **281**, 1333.
24 K. Shimizu, T. Kimura, S. Furomoto, K. Takeda, K. Kontani, Y. Onuki and K. Amaya, *Nature*, 2001, **412**, 316.
25 K. Shimizu, H. Ishikawa, D. Takao, T. Yagi and K. Amaya, *Nature*, 2002, **419**, 597; V. V. Struzhkin, M. I. Eremets, W. Gan, H.-k. Mao and R. J. Hemley, *Science*, 2002, **298**, 1213.
26 M. Debessai, J. J. Hamlin and J. S. Schilling, arXiv:0806.3407v1, 2008.
27 T. Yabuuchi, T. Matsuoka, Y. Nakamoto and K. Shimizu, *J. Phys. Soc. Jpn.*, 2006, **75**, 083703.
28 J. R. Gavaler, *Appl. Phys. Lett.*, 1973, **23**, 480.
29 H. S. Jeevan, Z. Hossain, C. Geibel and P. Gegenwart, arXiv:0807.2530v1, 2008.
30 S. Yamanaka, K.-i. Hotehama and H. Kawaji, *Nature*, 1998, **392**, 580.
31 J. Nagamatsu, N. Nakagawa, T. Muranaka, Y. Zenitani and J. Akimitsu, *Nature*, 2001, **410**, 63.
32 T. T. M. Palstra, O. Zhou, Y. Iwasa, P. E. Sulewski, R. M. Fleming and O. Zegarski, *Solid State Commun.*, 1995, **93**, 327.
33 See for example J. Yang, Z.-C. Li, W. Lu, W. Yi, X.-L. Shen, Z.-A. Ren, G.-C. Che, X.-L. Dong, L.-L. Sun, F. Zhou and Z.-X. Zhao, *Supercond. Sci. Technol.*, 2008, **21**, 082001; Y. Takabayashi, M. T. McDonald, D. Papanikolaou, S. Margadonna, G. Wu, R. H. Liu, X. H. Chen and K. Prassides, *J. Am. Chem. Soc.*, 2008, **130**, 9242; B. Lorenz, K. Sasmal, R. P. Chaudhury, X. H. Chen, R. H. Liu, T. Wu, and C. W. Chu, arXiv:0804.1582, 2008; H. Takahashi, K. Igawa, K. Arii, Y. Kamihara, M. Hirano and H. Hosono, *Nature*, 2008, **453**, 376 and references therein.
34 J. G. Bednorz and K. A. Müller, *Z. Phys. B*, 1986, **64**, 189.
35 M. K. Wu, J. R. Ashburn, C. J. Torng, P. H. Hor, R. L. Meng, L. Gao, Z. J. Huang, Y. Q. Wang and C. W. Chu, *Phys. Rev. Lett.*, 1987, **58**, 908.
36 P. Dai, B. C. Chakoumakos, G. F. Sun, K. W. Wong, Y. Xin and D. F. Lu, *Physica C*, 1995, **243**, 201.
37 L. Gao, Y. Y. Xue, F. Chen, Q. Xiong, R. L. Meng, D. Ramirez, C. W. Chu, J. H. Eggert and H.-k. Mao, *Phys. Rev. B*, 1994, **50**, 4260. T_C of 166 ± 1 K for fluorinated Hg1223 at 23 GPa has also been claimed: M. Monteverde, C. Acha, M. Núñez-Regueiro, D. A. Pavlov, K. A. Lokshin, S. N. Putilin and E. V. Antipov, *Europhys. Lett.*, 2005, **72**, 458.
38 This has sometimes been placed in doubt; see: J. D. Dow and D. R. Harshman, *Int. J. Mod. Phys. B*, 2007, **21**, 3086; J. D. Dow and D. R. Harshman, *J. Supercond.*, 2004, **17**, 179 and references therein.
39 Y. Tokura, H. Takagi and S. Uchida, *Nature*, 1989, **337**, 345.
40 J. D. Jorgensen, P. G. Radaelli, D. G. Hinks, J. L. Wagner, S. Kikkawa, G. Er and F. Kanamaru, *Phys. Rev. B*, 1993, **47**, 14654.
41 T. Kajita, M. Kato, T. Suzuki, T. Itoh, T. Noji and Y. Koike, *Jpn. J. Appl. Phys.*, 2004, **43**, L1480; T. Kajita, M. Kato, T. Suzuki, T. Itoh, T. Noji and Y. Koike, *Physica C*, 2005, **426**, 500.
42 H. A. Blackstead, J. D. Dow and M. Lehmann, *Int. J. Mod. Phys. B*, 1999, **13**, 3688.
43 See A. Bianconi, A. Congiu Castellano, M. De Santis, P. Rudolf, P. Lagarde, A. M. Flank and A. Marcelli, *Solid State Commun.*, 1987, **63**, 1009; G. Liang, Q. Yao, S. Zhou and D. Katz, *Physica C*, 2005, **424**, 107; N. Nücker and et al., *J. Supercond.*, 1999, **12**, 143, and references therein.
44 A. Fujimori, E. Takayama-Muromachi, Y. Uchida and B. Okai, *Phys. Rev. B*, 1987, **35**, 8814; A. Fujimori, E. Takayama-Muromachi and Y. Uchida, *Solid State Commun.*, 1987, **63**, 857.
45 See for example C. N. R. Rao, *Mod. Phys. Lett. B*, 1988, **2**, 1217; A. Fujimori, *Phys. Rev. B*, 1989, **39**, 793; I. I. Mazin and A. I. Liechtenstein, *Phys. Rev. B*, 1998, **57**, 150; W. A. Little, K. Collins and M. J. Holcomb, *J. Supercond.*, 1999, **12**, 89.
46 C. K. N. Patel and R. C. Dynes, *Proc. Natl. Acad. Sci. U. S. A.*, 1988, **85**, 4945.
47 C. N. R. Rao and A. K. Ganguli, *Chem. Soc. Rev.*, 1995, **24**, 1.
48 K. Fijałkowski and W. Grochala, *Dalton Trans.*, 2008, 5447.
49 T. Cuk, V. V. Struzhkin, T. P. Devereaux, A. F. Goncharov, C. A. Kendziora, H. Eisaki, H.-K. Mao and Z.-X. Shen, *Phys. Rev. Lett.*, 2008, **100**, 217003.
50 J. K. Burdett, *Inorg. Chem.*, 1993, **32**, 3915.
51 J. K. Burdett, *Acc. Chem. Res.*, 1995, **28**, 227.
52 R. S. Berry, *J. Chem. Phys.*, 1957, **27**, 1288.
53 A. Lanzara *et al.*, *Nature*, 2001, **412**, 510; T. Cuk, D. H. Lu, X. J. Zhou, Z.-X. Shen, T. P. Devereaux and N. Nagaosa, *Phys. Status Solidi B*, 2005, **242**, 11; L. Pintschovius, *Phys. Status Solidi B*, 2005, **242**, 30; M. Braden, L. Pintschovius, T. Uefuji and K. Yamada, *Phys. Rev. B*, 2005, **72**, 184517; M. d'Astuto, P. K. Mang, P. Giura, A. Shukla, P. Ghigna, A. Mirone, M. Braden, M. Greven, M. Krisch and F. Sette, *Phys. Rev. Lett.*, 2002, **88**, 167002; A. Gauzzi, M. d'Astuto, F. Licci, A. Bossak and M. Krisch, *Phys. Rev. B*, 2007, **75**, 144511, Compare also: X. J. Chen, V. V. Struzhkin, Z. Wu, R. J. Hemley and H. K. Mao, *Phys. Rev. B*, 2007, **75**, 134504; X. J. Chen, V. V. Struzhkin, Z. Wu, H. Q. Lin, R. J. Hemley and H. K. Mao, *Proc. Natl. Acad. Sci. U. S. A.*, 2007, **104**, 3732; O. Rösch and

O. Gunnarsson, *Phys. Rev. Lett.*, 2004, **92**, 146403; T. Egami, *J. Phys. Chem. Solids*, 2006, **67**, 50; K. A. Müller, *J. Phys.: Condens. Matter*, 2007, **19**, 251002; J. B. Goodenough, *J. Phys.: Condens. Matter*, 2003, **15**, R257.
54 S. Deng, A. Simon and J. Köhler, *J. Phys. Chem. Solids*, 2001, **62**, 1441; S. Deng, A. Simon and J. Köhler, *Struct. Bond.*, 2005, **114**, 103; A. Simon, *Solid State Sci.*, 2005, **7**, 1451.
55 J. Bardeen, L. N. Cooper and J. R. Schrieffer, *Phys. Rev.*, 1957, **108**, 1175.
56 T. Jaroń, W. Grochala and R. Hoffmann, *J. Mater. Chem.*, 2006, **16**, 1154. It is significant that avoided crossing seems to be important for such different superconducting materials as oxocuprates and samarium sulphide (SmS): C. M. Varma, *Rev. Mod. Phys.*, 1976, **48**, 218. Independent calculations confirm the hypothesis of dual character of the wavefunction for oxobismuthates as well: N. C. Pyper and P. P. Edwards, in: *Polarons and Bipolarons in High-T_C Superconductors and Related Materials*, ed. E. K. H. Salje, A. S. Alexandrov and W. Y. Liang, Cambridge University Press, Cambridge, 1995.
57 Compare for example: P. Monthoux, D. Pines and G. G. Lonzarich, *Nature*, 2007, **450**, 1177; A. Bussmann-Holder, *J. Supercond.*, 1999, **12**, 19; J. Hwang, T. Timusk and G. D. Gu, *Nature*, 2004, **427**, 714; R. S. Markiewicz, *J. Phys.: Condens. Matter*, 1994, **6**, 3059; R. Gatt and I. Panas, *Chem. Phys. Lett.*, 1997, **266**, 410; A. S. Moskvin, *JETP Lett.*, 2004, **80**, 697; E. Dagotto, A. Nazarenko, A. Moreo, S. Haas and M. Boninsegni, *J. Supercond.*, 1995, **8**, 483; B. Pradhan and G. C. Rout, *Physica C*, 2008, **468**, 72.
58 M. B. Robin and P. Day, *Adv. Inorg. Chem. Radiochem.*, 1967, **10**, 247.
59 P. F. Barbara, T. J. Meyer and M. A. Ratner, *J. Phys. Chem.*, 1996, **100**, 13148; I. B. Bersuker, V. Z. Polinger, *Vibronic Interactions in Molecules and Crystals*, Springer-Verlag: Berlin, 1989; K. Y. Wong, P. N. Schatz, A Dynamic Model for Mixed-Valence Compounds, in: *Progress in Inorganic Chemistry*, ed. S. J. Lippard, Wiley, New York, 1981, vol. 28, p. 369; I. B. Bersuker, *The Jahn–Teller Effect and Vibronic Interactions in Modern Chemistry*, Plenum Press, New York, 1984; I. B. Bersuker, *Electronic structure and properties of transition metal compounds: introduction to the theory*, Wiley, New York, 1996.
60 W. Grochala, R. Konečny and R. Hoffmann, *Chem. Phys.*, 2001, **265**, 153.
61 W. Grochala and R. Hoffmann, *New J. Chem.*, 2001, **25**, 108.
62 W. Grochala and R. Hoffmann, *J. Phys. Chem. A*, 2000, **104**, 9740.
63 W. Grochala and R. Hoffmann, *Pol. J. Chem.*, 2001, **75**, 1603.
64 W. Grochala, A. C. Albrecht and R. Hoffmann, *J. Phys. Chem. A*, 2000, **104**, 2195.
65 W. Grochala, *J. Mol. Model.*, 2005, **11**, 323.
66 W. Grochala, R. Hoffmann and P. P. Edwards, *Chem. Eur. J.*, 2003, **9**, 575.
67 M. Atanasov and D. Reinen, *J. Phys. Chem. A*, 2001, **105**, 5450; M. Atanasov and D. Reinen, *J. Am. Chem. Soc.*, 2002, **124**, 6693; M. Atanasov and D. Reinen, *Adv. Quant. Chem.*, 2003, **44**, 355; M. Atanasov and D. Reinen, *Inorg. Chem.*, 2004, **43**, 1998; M. Atanasov and D. Reinen, *Inorg. Chem.*, 2005, **44**, 5092.
68 Compare: A. W. Sleight, *Acc. Chem. Res.*, 1995, **28**, 103; J. C. Phillips, *Phys. Rev. Lett.*, 1972, **29**, 1551; J. E. Moussa and M. L. Cohen, *Phys. Rev. B: Condens. Matter Mater. Phys.*, 2008, **78**, 064502.
69 A. Rehr and M. Jansen, *Inorg. Chem.*, 1992, **31**, 4740.
70 T. Drews and K. Seppelt, *Angew. Chem., Int. Ed. Engl.*, 1997, **36**, 273.
71 J. Grannec, L. Lozano, J. Portier and P. Hagenmüller, *Z. Anorg. Allg. Chem.*, 1971, **385**, 26.
72 J. Koehler and J.-H. Chang, *Z. Anorg. Allg. Chem.*, 1997, **623**, 596; J. C. Taylor and P. W. Wilson, *J. Am. Chem. Soc.*, 1973, **95**, 1834.
73 N. Ruchaud, C. Mirambet, L. Fournes and J. Grannec, *Z. Anorg. Allg. Chem.*, 1990, **590**, 173; M. F. A. Dove, R. King and T. J. King, *Chem. Commun.*, 1973, 944.
74 N. Nguyen, P. Plurien, H. Marquet Ellis and P. Charpin, *C. R. Ser. C*, 1972, **275**, 1503.
75 W. A. S. Nandana, J. Passmore, D. C. N. Swindells, P. Taylor, P. S. White and J. E. Vekris, *J. Chem. Soc., Dalton Trans.*, 1983, 619; W. A. S. Nandana, J. Passmore and P. S. White, *J. Chem. Soc., Dalton Trans.*, 1985, 1623; W. A. S. Nandana, J. Passmore, P. S. White and C. M. Wong, *J. Chem. Soc., Dalton Trans.*, 1987, 1989; R. Minkwitz and J. Nowicki, *Z. Anorg. Allg. Chem.*, 1991, **605**, 109; J. Fawcett, J. H. Holloway, D. R. Russell, A. J. Edwards and K. I. Khallow, *Can. J. Chem.*, 1989, **67**, 2041; R. J. Gillespie, D. R. Slim and J. E. Vekris, *J. Chem. Soc., Dalton Trans.*, 1977, 971.
76 P. Day, C. Vettier and G. Parisot, *Inorg. Chem.*, 1978, **17**, 2319 and ref. 11 therein.
77 See for example: T. Hattori, T. Idogaki and N. Uryu, *Phys. Status Solidi B*, 1988, **148**, K47; J. Darriet, J. L. Soubeyroux, H. Touhara, A. Tressaud and P. Hagenmüller, *Mater. Res. Bull.*, 1982, **17**, 315; S. P. Gabuda, V. N. Ikorskii, S. G. Kozlova and P. S. Nikitin, *JETP Lett.*, 2001, **73**, 35.
78 W. J. Casteel Jr, D. H. Lohmann and N. Bartlett, *J. Fluorine Chem.*, 2001, **112**, 165; W. J. Casteel Jr, A. P. Wilkinson, H. Borrmann, R. E. Serfass and N. Bartlett, *Inorg. Chem.*, 1992, **31**, 3124.
79 J. Chassaign and D. Bizot, *J. Fluorine Chem.*, 1980, **16**, 451; H. Schaefer, H. G. von Schnering, K. J. Niehues and H. G. Nieder Vahrenholz, *J. Less Common Met.*, 1965, **9**, 95.
80 R. Hoppe and S. Becker, *Z. Anorg. Allg. Chem.*, 1989, **568**, 126.
81 T. Moriya, *Phys. Rev.*, 1960, **120**, 91; G. K. Wertheim, H. J. Guggenheim and D. N. E. Buchanan, *Phys. Rev.*, 1968, **169**, 465.
82 B. J. Kennedy and T. Vogt, *Mater. Res. Bull.*, 2002, **37**, 77.
83 B. Žemva, K. Lutar, L. Chachón, M. Fele-Beuermann, J. Allman, C. Shen and N. Bartlett, *J. Am. Chem. Soc.*, 1995, **117**, 10025.
84 A. L. Hector, E. G. Hope, W. Levason and M. T. Weller, *Z. Anorg. Allg. Chem.*, 1998, **624**, 1982; A. Tressaud, M. Wintenberger, N. Bartlett and P. Hagenmüller, *C. R. Acad. Sci. Paris, Serie C*, 1976, **282**, 1069.
85 J. Strempfer, U. Rütt, S. P. Bayrakci, Th. Brückel and W. Jauch, *Phys. Rev. B*, 2004, **69**, 014417.
86 See J. Strempfer, U. Rütt and W. Jauch, *Phys. Rev. Lett.*, 2001, **86**, 3152 and references therein.
87 N. Morita, T. Endo, T. Sato and M. Shimada, *J. Mater. Sci. Lett.*, 1987, **6**, 859.
88 F. Ebert, *Z. Anorg. Allg. Chem.*, 1931, **196**, 395; N. Bartlett and R. Maitland, *Acta Crystallogr.*, 1958, **11**, 747; R. P. Rao, R. C. Sherwood and N. Bartlett, *J. Chem. Phys.*, 1968, **49**, 3728; D. Paus and R. Hoppe, *Z. Anorg. Allg. Chem.*, 1977, **431**, 207.
89 Z. Mazej, A. Tressaud and J. Dariett, *J. Fluorine Chem.*, 2001, **110**, 139, This cubic $Pa\bar{3}$ form is isostructural with the high-pressure form: B. G. Müller, *J. Fluorine Chem.*, 1982, **20**, 291; A. Tressaud, J. L. Soubeyroux, H. Touhara, G. Demazeau and F. Langlais, *Mater. Res. Bull.*, 1981, **16**, 207.
90 See P. Reinhardt, I. de P. R. Moreira, C. de Graaf, R. Dovesi and F. Illas, *Chem. Phys. Lett.*, 2000, **319**, 625 and references therein. For structural details, see: J. C. Taylor and P. W. Wilson, *J. Less Common Met.*, 1974, **34**, 257. Compare with: P. Fischer, W. Hälg, D. Schwarzenbach and H. Gamsjäger, *J. Phys. Chem. Solids*, 1974, **35**, 1683 where FM ordering of CuF_2 has been discussed.
91 P. Charpin, A.-J. Dianoux, H. Marquet-Ellis and C. Nguyen-Nghi, *Compt. Rend. Seances Acad. Sci. Ser. B*, 1966, **263**, 1359; A. Jesih, K. Lutar, B. Žemva, B. Bachmann, S. Becker, B. G. Müller and R. Hoppe, *Z. Anorg. Allg. Chem.*, 1990, **588**, 77. Compare with report on erroneously assigned monoclinic structure of AgF_2: E. A. Baturina, Y. A. Lukyanychev and L. N. Rastorguev, *Zh. Strukt. Khim.*, 1966, **7**, 627.
92 P. Fisher, D. Schwarzenbach and H. M. Rietveld, *J. Phys. Chem. Solids*, 1971, **32**, 543; P. Fisher, G. Roult and D. Schwarzenbach, *J. Phys. Chem. Solids*, 1971, **32**, 1641. Compare with report on (erroneously assigned) AFM properties of AgF_2: T. J. Bastow, H. J. Whitfield and R. W. Cockman, *Solid State Commun.*, 1981, **39**, 325.
93 D. Kurzydłowski and W. Grochala, *Chem. Commun.*, 2008, 1073.
94 S. Ido, S. Uchida, K. Kitazawa and S. Tanaka, *J. Phys. Soc. Jpn.*, 1988, **57**, 997; M. B. Robin, K. Andres, T. H. Geballe, N. A. Kuebler and D. B. McWhan, *Phys. Rev. Lett.*, 1966, **17**, 917.
95 W. Grochala and R. Hoffmann, *Angew. Chem., Int. Ed.*, 2001, **40**, 2742; B. G. Müller, *Angew. Chem., Int. Ed. Engl.*, 1987, **26**, 1081.
96 P. Malinowski, Z. Mazej and W. Grochala, *Z. Anorg. Allg. Chem.*, 2008, **634**, 2608.
97 D. Grzybowska, P. Malinowski, Z. Mazej and W. Grochala, *Collect. Czech. Chem. Commun.*, 2008, **73**, 1729.
98 A. A. Goryunkov, V. Yu. Markov, O. V. Boltalina, B. Žemva, A. K. Abdul-Sada and R. Taylor, *J. Fluorine Chem.*, 2001, **112**, 191.

99 G. Cady, A. Grosse, E. Barber, L. Burger and Z. Sheldon, *Ind. Eng. Chem.*, 1947, **39**, 290, see also: F. Aubke, *J. Fluorine Chem.*, 1995, **71**, 199; S. Rosen, *Acc. Chem. Res.*, 1988, **21**, 307.
100 B. Žemva, R. Hagiwara, W. J. Casteel Jr, K. Lutar, A. Jesih and N. Bartlett, *J. Am. Chem. Soc.*, 1990, **112**, 4846; B. Žemva and N. Bartlett, *J. Fluorine Chem.*, 2006, **127**, 1463.
101 *Comprehensive Inorganic Chemistry*, ed. J. C. Bailar, H. J. Emeleus, R. Nyholm and A. F. Trotman-Dickenson, Oxford, Pergamon Press, 1973, p. 1053.
102 H. Firouzabadi, P. Salehi and I. Mohammadpour-Baltork, *Bull. Chem. Soc. Jpn.*, 1992, **65**, 2878.
103 W. Grochala, *J. Fluorine Chem.*, 2008, **129**, 82.
104 W. Grochala, *Phys. Status Solidi B*, 2006, **243**, R81. It should be understood that by 'normal' Jahn–Teller distortion for an octahedral d^9 complex we mean elongation of the octahedron, which is the typical case for an isolated complex in the gas phase. *Cf.* ref. 110.
105 J. Gažo, I. B. Bersuker, J. Garaj, M. Kabešová, J. Kohout, H. Langfelderová, M. Melnik, M. Serátor and F. Valach, *Coord. Chem. Rev.*, 1976, **19**, 253, Compare also: G. Landrum and R. Hoffmann, *Angew. Chem., Int. Ed.*, 1998, **37**, 1887.
106 W. Grochala, R. G. Egdell, P. P. Edwards, Z. Mazej and B. Žemva, *ChemPhysChem*, 2003, **4**, 997.
107 It is anticipated that metal–F bonding will be somewhat less covalent for connections of divalent gold than those of divalent silver. This is because relativistic effects render 5d electrons of Au less bound (softer, more diffuse, easier to ionize) than the 4d electrons of Ag. In a sense, lighter silver is 'not relativistic enough'.
108 In principle, the energy of a ligand's frontier orbitals with respect to those of metal centers determine the fate of metal comproportionation/disproportionation. For the importance of a ligand's LUMO in certain Ru^{3+}/Ru^{4+} complexes, see: S. Ernst, V. Kasack and W. Kaim, *Inorg. Chem.*, 1988, **27**, 1146; W. Kaim and V. Kasack, *Inorg. Chem.*, 1990, **29**, 4696.
109 Unrestricted B3LYP single-point energy calculation with 6-311++G** basis for F, SDDAll relativistic pseudopotentials and double zeta valence electron basis for Ag. All Ag–F distances have been kept at 2.00 Å to mimic the situation found in hypothetical tetragonal $[AgF_{4/2}]$ lattices.
110 H. L. Schläfer, and G. Gliemann, *Basic Principles of Ligand Field Theory*, Wiley Interscience, New York, 1969. It should be remembered that the value of 10 Dq des not reflect directly the covalence in a transition metal complex. It has been pointed out that there are *two* contributions to 10 Dq related to chemical bonding; in particular for F^- one of these contributions reflects the admixture of deep-lying 2s levels of F into the antibonding e_g orbital. See for example: M. Moreno, M. T. Barriuso, J. A. Aramburu1, P. García-Fernández and J. M. García-Lastra, *J. Phys.: Condens. Matter*, 2006, **18**, R315.
111 S. E. McLain, M. R. Dolgos, D. A. Tennant, J. F. C. Turner, T. Barnes, T. Proffen, B. C. Sales and R. I. Bewley, *Nat. Mater.*, 2006, **5**, 561.
112 Z. Mazej *et al.*, *Cryst. Eng. Commun.*, 2009, DOI: 10.1039/b902161b.
113 W. Grochala, *Nat. Mater.*, 2006, **5**, 513.
114 T. Lancaster, S. J. Blundell, P. J. Baker, W. Hayes, S. R. Giblin, S. E. McLain, F. L. Pratt, Z. Salman, E. A. Jacobs, J. F. C. Turner and T. Barnes, Phys. Rev. B, 2007, **75**, 220408(R).
115 J. Saylor, L. Takacs, C. Hohenemser, J. I. Budnick and B. Chamberland, *Phys. Rev. B*, 1989, **40**, 6854; B. Keimer, A. Aharony, A. Auerbach, R. J. Birgeneau, A. Cassanho, Y. Endoh, R. W. Erwin, M. A. Kastner and G. Shirane, *Phys. Rev. B*, 1992, **45**, 7430.
116 H. Wu and D. I. Khomskii, *Phys. Rev. B*, 2007, **76**, 155115; E.-J. Kan, L.-F. Yuan, J. Yang and J. G. Hou, *Phys. Rev. B*, 2007, **76**, 024417.
117 T. Jaroń and W. Grochala, *Phys. Status Solidi RRL*, 2008, **2**, 71.
118 W. J. Casteel, Jr., G. Lucier, R. Hagiwara, H. Borrmann and N. Bartlett, *J. Solid State Chem.*, 1992, **96**, 84; G. Lucier, J. Münzenberg, W. J. Casteel, Jr. and N. Bartlett, *Inorg. Chem.*, 1995, **34**, 2692.
119 C. P. Shen, B. Žemva, G. M. Lucier, O. Graudejus, J. A. Allman and N. Bartlett, *Inorg. Chem.*, 1999, **38**, 4570.
120 W. Grochala and P. P. Edwards, *Phys. Status Solidi B*, 2003, **240**, R11.
121 T. Jaroń, W. Grochala and R. Hoffmann, *Phys. Status Solidi B*, 2005, **242**, R1. This early study used the old crystal structure of $KAgF_3$ taken from: R. H. Odenthal and R. Hoppe, *Monatsh. Chem.*, 1971, **102**, 1340.
122 W. Grochala, A. Porch and P. P. Edwards, *Solid State Commun.*, 2004, **130**, 137.
123 W. Grochala, J. Feng, R. Hoffmann and N. W. Ashcroft, *Angew. Chem., Int. Ed.*, 2007, **46**, 3620.
124 S. Hull and P. Berastegui, *J. Phys.: Condens. Matter*, 1998, **10**, 7945; Y. Li, L. J. Zhang, T. Cui, Y. W. Li, Y. M. Ma, Z. He and G. T. Zou, *J. Phys.: Condens. Matter*, 2007, **19**, 425217.
125 J. Romiszewski, W. Grochala and L. Stolarczyk, *J. Phys. Cond. Matter*, 2006, **19**, 116206.
126 T. Jaroń and W. Grochala, *2nd Workshop on ab initio phonon calculations*, Cracow, Poland, 6–8 December 2007.
127 H. Müller-Buschbaum, *Z. Anorg. Allg. Chem.*, 2004, **630**, 2125.
128 In the gas phase, the ground state of '$AgCl_2$' could be described as Ag(I) bound to two chloride anions with one hole shared by their p/p orbitals: H. C. Müller-Rösing, A. Schulz and M. Hargittai, *J. Am. Chem. Soc.*, 2005, **127**, 8133.
129 P. C. Leung and F. Aubke, *Inorg. Chem.*, 1978, **17**, 1765; P. C. Leung, K. C. Lee and F. Aubke, *Can. J. Chem.*, 1979, **57**, 326.
130 P. Malinowski, Z. Mazej and W. Grochala, *5th School of Thermal Analysis SAT'08*, Zakopane, Poland, 6–9 April 2008; P. Malinowski, Z. Mazej and W. Grochala, *E-MRS Fall Meeting*, Warsaw, Poland, 15–19 September 2008.
131 W. Grochala, *Inorg. Chem. Commun.*, 2008, **11**, 155.
132 J. A. McMillan, *Chem. Rev.*, 1962, **62**, 65.
133 G. B. Kauffman, R. A. Houghten, R. E. Likins, P. L. Posson, R. K. Ray, J. P. Fackler Jr. and R. T. Stubbs, in: *Inorganic Syntheses*, ed. M. Y. Darensbourg, vol. 32, 1998, p. 177 (and references therein); R. S. Bannerjee and S. Basu, *J. Inorg. Nucl. Chem.*, 1964, **26**, 821.
134 E. K. Barefield and M. T. Mocella, *Inorg. Chem.*, 1973, **12**, 2829; Q.-M. Wang and T. C. W. Mak, *Chem. Commun.*, 2001, 807; Q.-M. Wang, H. K. Lee and T. C. W. Mak, *New J. Chem.*, 2002, **26**, 513.
135 A. Malaguti, *Ann. Chim. (Rome)*, 1955, **41**, 251.
136 I. Zilbermann, J. Hayon, E. Maimon, R. Ydgar, E. Korin and A. Bettelheim, *Electrochem. Commun.*, 2002, **4**, 862; H. Kunkely and A. Vogler, *Inorg. Chem. Commun.*, 2007, **10**, 479.
137 J. L. Shaw, J. Wolowska, D. Collison, J. A. K. Howard, E. J. L. McInnes, J. McMaster, A. J. Blake, C. Wilson and M. Schrőder, *J. Am. Chem. Soc.*, 2006, **128**, 13827; D. Huang, A. J. Blake, E. J. L. McInnes, J. McMaster, E. S. Davies, C. Wilson, J. Wolowska and M. Schröder, *Chem. Commun.*, 2008, 1305.
138 J. Darriet, M. S. Haddad, E. N. Duesler and D. N. Hendrickson, *Inorg. Chem.*, 1979, **18**, 2679; T. Lancaster *et al.*, *Phys. Rev. B*, 2007, **75**, 094421.
139 R. W. Matthews and R. A. Walton, *Inorg. Chem.*, 1971, **10**, 1433.
140 L. Puškar, H. Cox, A. Goren, G. D. C. Aitken and A. J. Stace, *Faraday Discuss.*, 2003, **124**, 259.
141 W. Grochala, *J. Mol. Model.*, 2008, **14**, 887.
142 D. Grzybowska, Z. Mazej and W. Grochala, *15th European Symposium on Fluorine Chemistry*, Prague, Czech Republic, 15–20 July 2007.
143 J. Y. Kim, A. J. Norquist and D. O'Hare, *Chem. Commun.*, 2002, 2198.
144 R. J. Francis, P. S. Halasyamani and D. O'Hare, *Chem. Mater.*, 1998, **10**, 3131.
145 Hydrothermal synthesis is used to generate UFO and TFO but it is certainly not possible if starting from AgF_2 because of the extreme sensitivity of this compound towards moisture.
146 C. K. Jùrgensen, *Mol. Phys.*, 1959, **2**, 309.
147 Ag(II) easily oxidizes Cl^- anions; Cu(II) does the same to I^-.
148 W. Grochala, *Scr. Mater.*, 2006, **55**, 811.
149 Unrestricted B3LYP calculations with 6-311++G** basis for F, LANL relativistic pseudoptentials and double zeta valence electron basis for Ag.
150 S. Larsson, *Chem. Eur. J.*, 2004, **10**, 5277.
151 J. L. Manson, K. H. Stone, H. I. Southerland, T. Lancaster, A. J. Steele, S. J. Blundell, F. L. Pratt, P. J. Baker, R. D. McDonald, P. Sengupta, J. Singleton, P. A. Goddard, C. Lee, M.-H. Whangbo, M. M. Warter, C. H. Mielke and P. W. Stephens, *J. Am. Chem. Soc.*, 2009, **131**, 4590.

